UNIVERSIDADE DE LISBOA

FACULDADE DE CIÊNCIAS

DEPARTAMENTO DE FÍSICA

Synchronization of Coupled Oscillators

Paulo José Severino Maurício

Mestrado em Física

Especialização Física Estatística e Não Linear

2010

UNIVERSIDADE DE LISBOA

FACULDADE DE CIÊNCIAS

DEPARTAMENTO DE FÍSICA

Synchronization of Coupled Oscillators

Paulo José Severino Maurício

Dissertação sob a orientação de

Professora Ana Nunes (FCUL, Centro de Física da Matéria Condensada do CI da UL)

Professor Pedro Freitas (FMH, Grupo de Física-Matemática do CI da UL)

Mestrado em Física

Especialização Física Estatística e Não Linear

2010

Contents

Abstract

In this work we begin by introducing the Kuramoto model, constructing its solutions in the thermodynamic limit and showing the close connection between statistical physics and dynamical systems that lead to the main theoretical insights. The systematic study of a finite population of self sustained oscillators began in the first decade of this century. Unlike most of the papers we have found, we are not interested in the synchronization transition in itself but rather in phase locked patterns and their relation with frequency distribution among oscillators.

The problem of stability, as we have already mentioned, experienced great advances in recent years. In a brief discussion we only address the problem of stability of the simplest solution allowed by the Kuramoto model: the incoherent solution. After that we introduce chimera states, first noticed by Kuramoto and his colleagues ([17] and references therein), in which the introduction of a non local coupling gives origin to a split in a region with synchronised oscillators and other with asynchronous one.

Then we proceed by exploring the literature and the results with a finite number of oscillators, field explored with persistence only since mainly 2004 [29]. But here we are yet in Kuramoto framework which is abandoned, in a rigorous terminology, when we pursuit structured and not all-to-all coupling. Although we could introduce the same mean fields quantities if well defined in each situation, this did not help us in making sense of the results and is not an help in any analytical work.

In our analysis of a ring of coupled oscillators we construct a space that allows us to relate the stable solutions with the eigenvectors of the laplacian of the graph in which we work.

Resumo

Neste trabalho começamos por introduzir o modelo de Kuramoto e realizar a construção das suas soluções no limite termodinâmico, mostrando a relação estreita entre física estatística e sistemas dinâmicos que levaram aos desenvolvimentos mais significativos.

O estudo sistemático das populações de osciladores com um número finito de elementos começaram na primeira década deste século. Ao contrário de muitos trabalhos nesta área, não estamos interessados no processo de sincronização em si mas antes em padrões de fases que surgem em sincronia e sua relao com a distribuição das frequências próprias entre osciladores.

O problema da estabilidade das soluções teve grandes desenvolvimento nos últimos anos. Numa breve análise apenas atendemos ao problema da estabiliadde da mais simples solução do modelo de kuramoto: a solução incoerente. Depois introduzimos as *quimeras*, estados de sincronização descobertos por Kuramoto e que resultam da introdução de acoplamento não local, resultando numa separação entre uma zona de sincronia e uma zona assíncrona num mesmo sistema. Prosseguimos analisando a literatura e os resultados conhecidos com um número finito de osciladores, um campo explorado de forma sistemática apenas após, *grosso modo*, 2004. Abandonamos o modelo de Kuramoto quando passamos ao estudo de um número finito de osciladores e introduzimos acoplamentos estruturados saindo do acoplamento de todos com todos. Nesta situação as quantidades de campo médio, na horigem do êxito do modelo de Kuramoto, ficam sem utilidade evidente, ainda que caso a caso se possam ainda definir e trabalhar.

A nossa análise num círculo onde os osciladores acoplam entre primeiros vizinhos e construimos um espaço onde podemos visualizar a relao entre as soluções estáveis e os vectores próprios do operador Laplaciano do grafo associado.

Acknowledgments

Chapter 1

Introduction

Synchronization is present in almost all branches of science, engineering and social sciences and is displayed in a variety of phenomena that appear to be rather different but nevertheless obey universal laws [1, 2] . Any group of systems, be it physical, biological or social that displays some rhythm, that is, some time periodicity can, under certain circumstances synchronize.

The broad occurrence of synchronization in nature is linked to the periodicity of the systems behaviour. However synchronization is always what is called an emergent property of an ensemble of units that exhibit some rhythm and are somehow in connection with each other. The heart must beat at a given determined pace, insulin-secreting cells of the pancreas must act in unison, and cells in the mammalian small intestine act to originate a wave. Even individual bacteria display circadian synchrony [3, 7]. These are examples of synchronization phenomena at a cellular level. For synchronization phenomena in biological systems we refer to the beautiful and well informed book *The Geometry of Biological Time* by Arthur Winfree, a delight to reason and knowledge.

Synchronization was discovered by the Dutch physicist Christian Huygens (1629-1695) when he noticed that two mechanical pendulums hanging from the same wall oscillate in phase opposition. He named it *"sympathy of two clocks"*. In a letter to his father dated from 26 February 1665 he wrote [1]:

> While I was forced to stay in bed for a few days and made observations on my two clocks [...], I noticed a wonderful effect that nobody could have thought before. The two clocks, while hanging [on the wall] side by side with a distance of one or two feet between, kept in pace relative to each other with a precision so high that the two pendulums always swung together, and never varied.

In the literature, synchronization phenomena are widely illustrated: flashing fireflies, chirp of crickets, epilepsy, menstrual period in groups of women, rhythmic applause, arrays of lasers and superconducting Josephson junctions are some of the myriad phenomena that display or are the result of a synchronization of cells, physical devices or biological

populations.

The seminal works of A. Andronov [4] on self sustained oscillators, of Norbert Wiener [5] on problems involving millions of limit cycle oscillators and showing the pervasiveness of synchrony in nature, of Arthur Winfree [3] in the first serious and fruitful approach to the problem and Kuramoto's work [11] in 1984 that establishes a theoretically and computational manageable model, can be seen as the main steps in the modern study of synchrony.

We must note that before the mid seventies of last century, it would be very unlikely, if not impossible at all, for a successful model to appear. In fact most of the success in the field emerges from a close connection between theory and computational work, each one giving insights to the other.

The very recent papers by Mirollo and Strogatz [13, 14] and by Ott and Antonsen [15, 16] that succeeded, respectively, in establishing the stability of partially locked and locked states of Kuramoto model, and the global stability of the system - but only for the case of a Lorentzian distribution of frequencies - have solved the main mathematical problems of the Kuramoto model.

In this work we begin by introducing the Kuramoto model, constructing its solutions in the thermodynamic limit and showing the close connection between statistical physics and dynamical systems that lead to the main theoretical insights. The assumption of an infinite number of oscillators, that is usually called in a loose terminology the thermodynamic limit, was, until recently [29] the framework of all the analytic studies. The systematic study of a finite population of self sustained oscillators began in the first decade of this century ([29] and reference [12] therein). Unlike most of the work mentioned in the literature, we are not interested in the synchronization transition in itself but rather in phase locked patterns and their relation with frequency distribution among oscillators.

The problem of stability, as we have already mentioned, experienced great advances in recent years. In a brief discussion we only address the problem of stability of the simplest solution allowed by the Kuramoto model: the incoherent solution. After that we introduce chimera states, first noticed by Kuramoto and his colleagues ([17] and references therein), in which the introduction of a nonlocal coupling gives origin to a split in a region with synchronized oscillators and other with asynchronous one.

We then consider the case of a finite number of oscillators, an area which started to receive more attention only recently [29]. Up to a point, this is still done within the Kuramoto framework, which is then abandoned when we consider structured and not all-to-all coupling. In this context, and although in some situations it might still be possible to try to apply some of the concepts and techniques that were useful before, it also becomes clear that there is still much to be understood and that some new ideas are needed. With the final part of this thesis, we hope to have started pointing in this direction.

7

Chapter 2

Standard Kuramoto Model

2.1 Kuramoto Model

The celebrated Kuramoto model [6, 9] of coupled phase oscillators has a phase equation of the form

$$\dot{\theta}_i(t) = \omega_i + \frac{K}{N} \sum_{j=1}^{N} \sin(\theta_j(t) - \theta_i(t)), \quad i = 1, ..., N, \tag{2.1}$$

where we consider N oscillators with natural frequencies ω_i, $i = 1, ..., N$ distributed with a given probability density $g(\omega)$, and K is the homogeneous all-to-all coupling constant.

Following Kuramoto [6], we assume that the probability density $g(\omega)$ is unimodal and symmetric about its mean frequency $\bar{\omega} = \int \omega g(\omega) d\omega$. We can always shift the mean of $g(\omega)$ to 0 by changing to a rotating frame at frequency $\bar{\omega}$. Defining a complex-valued order parameter

$$r(t)e^{i\psi(t)} = \frac{1}{N} \sum_{j=1}^{N} e^{i\theta_j(t)}, \tag{2.2}$$

where $0 \leqslant r(t) \leqslant 1$ measures the coherence of the oscillators, and $\psi(t)$ the average phase, we can write Eq.(2.1) in a more convenient way if we multiply both sides of Eq.(2.2) by $e^{-i\theta_i(t)}$

$$r(t)e^{i(\psi(t)-\theta_i(t))} = \frac{1}{N} \sum_{j=1}^{N} e^{i(\theta_j(t)-\theta_i(t))}. \tag{2.3}$$

Equating imaginary parts and using Eq.(2.1) we get

$$\dot{\theta}_i(t) = \omega_i + Kr(t)\sin(\psi(t) - \theta_i(t)), \quad i = 1, ..., N. \tag{2.4}$$

In this form the mean field character of the model becomes clear with each oscillator appearing to be decoupled from all the others, although they interact *via* the mean field
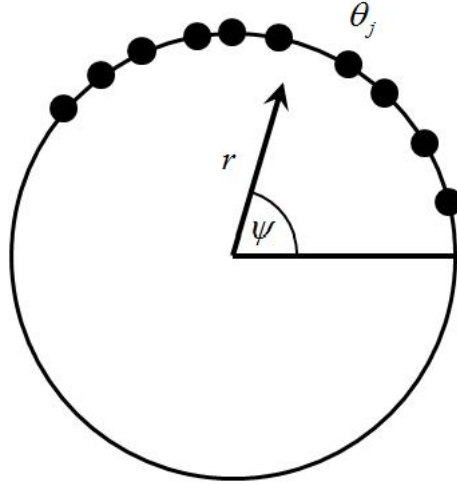
Figure 2.1: Geometric interpretation of the order parameter Eq.(2.2). The phases θ_j are plotted on the unit circle. Their centroid is given by the complex number $re^{i\psi}$, shown as an arrow.

quantities r and ψ. This is a very familiar approach in statistical physics, where the onset of synchrony from incoherence is viewed as a phase transition of the whole system of oscillators described by an order parameter.

After long years of mathematical and physical dead-ends,this approach to the problem revealed to be very fruitful combined with the analysis of the thermodynamic limit $N \rightarrow +\infty$. In this approximation, we treat the system of oscillators in the continuum limit, which provides a more manageable mathematical framework, sustained by the fact that oscillators in nature appear in large quantities: large amounts of fireflies or cells in biological pacemakers.

For a greater insight into the behaviour of the system it is also useful to represent graphically the meaning of the order parameter, Eq.(2.2). If all oscillators are put on a unit circle, circling around at given frequencies, we can see the order parameter r as the length of an arrow going from the centre of the unit circle to the centroid of the set of points that represent the oscillators. Clearly, $r \in [0,1]$ measures the coherence of the N oscillators. In the continuum limit this picture does not lose its meaning, taking the oscillators as continuously distributed on the unit circle.

2.1.1 Solutions of Kuramoto Model in the Thermodynamic Limit

In the thermodynamic limit $N \rightarrow +\infty$, oscillators are considered to be distributed with a probability density $\rho(\theta, \omega, t)$ where θ its the phase, ω the uncoupled frequency and t is

9

stands for time, satisfying the normalisation condition

$$\int_0^{2\pi} \rho(\theta, \omega, t)d\theta = 1, \tag{2.5}$$

and the arithmetic mean in Eq.(2.2) becomes an average over phase and frequency

$$r(t)e^{i\psi(t)} = \int_0^{2\pi} \int_{-\infty}^{+\infty} e^{i\theta}\rho(\theta, \omega, t)g(\omega)d\omega d\theta. \tag{2.6}$$

Now we will show that we get a variation of $r(t)$ from 0 to 1 when K goes from 0 to ∞. That is, the system of oscillators evolves from complete incoherence to complete synchrony as the coupling is turned on and its strength is taken to arbitrary large values.

When $K \to 0$, Eq.(2.4) yields $\theta_i(t) \approx \omega_i t + \theta_i(0)$ which means that without coupling each oscillator is free to rotate at his own frequency. Setting $\theta(t) = \omega t + \theta(0)$ in Eq.(2.6) we get

$$r(t)e^{i\psi(t)} = \int_0^{2\pi} \int_{-\infty}^{+\infty} e^{i(\omega t + \theta)}\rho(\theta, \omega, 0)g(\omega)d\omega d\theta. \tag{2.7}$$

Developing the exponential and rearranging the integrals yields

$$r(t)e^{i\psi(t)} = \int_{-\infty}^{+\infty}\left(\int_0^{2\pi}\cos(\omega t + \theta)\rho(\theta, \omega, 0)d\theta\right)g(\omega)d\omega +$$

$$+ i\int_{-\infty}^{+\infty}\left(\int_0^{2\pi}\sin(\omega t + \theta)\rho(\theta, \omega, 0)d\theta\right)g(\omega)d\omega \tag{2.8}$$

Since $\rho(\theta, \omega, 0)$ is integrable on $[0, 2\pi]$, we are in the conditions of the Riemann-Lebesgue Lemma, and so both terms on the right hand side of Eq.(2.8) tend to zero when $t \to \infty$. Thus we have seen that for $K \to 0$ and in the limit $t \to \infty$ we get $r \to 0$.

On the other hand, as $K \to \infty$ all the oscillators become phase locked in their average phase, $\theta_i(t) \approx \psi(t)$. In fact, if we rearrange Eq.(2.4) in the more convenient form

$$\frac{\dot{\theta}(t) - \omega_i}{Kr(t)} = \sin(\psi(t) - \theta_i(t)), \tag{2.9}$$

in the limit $K \to \infty$ we get $\sin(\psi(t) - \theta_i(t)) \to 0$ or $\theta_i(t) \to \psi(t)$. Using (2.6) yields

$$r(t)e^{i\psi(t)} = e^{i\psi(t)}\int_0^{2\pi}\int_{-\infty}^{+\infty}\rho(\theta, \omega, 0)g(\omega)d\omega d\theta. \tag{2.10}$$

But these integrals are equal to unity since they are integrals of densities over all range, so we get $r \to 1$.

We have seen that we get a variation of $r(t)$ from 0 to 1 when K goes from $K = 0$ to $K = \infty$, that is, the system of oscillators evolves from complete incoherence to complete synchrony.

Let us now study in more detail the nature of this transition. In the thermodynamic limit we have the continuity equation for the oscillator density $\rho(\theta, \omega, t)$

$$\frac{\partial \rho}{\partial t} + \frac{\partial}{\partial \theta}[\rho(\theta, \omega, t)v(\theta, \omega, t)] = 0, \tag{2.11}$$

which expresses conservation of oscillators of frequency ω and where the velocity v is interpreted as the instantaneous phase velocity of an oscillator with phase θ, given that it has natural frequency ω,

$$v(\theta, \omega, t) = \omega + Kr(t)\sin(\psi(t) - \theta). \tag{2.12}$$

This equation, being formally equivalent to (2.4) is its counterpart in the thermodynamic limit. For a more convenient expression we substitute Eq.(2.12) into Eq.(2.11) getting

$$\frac{\partial \rho(\theta, \omega, t)}{\partial t} + \frac{\partial}{\partial \theta}\{\rho(\theta, \omega, t)[\omega + Kr(t)\sin(\psi(t) - \theta)]\} = 0. \tag{2.13}$$

Let us focus on *stationary* solutions. The set of Eqs.(2.5),(2.6) and (2.13) has the trivial stationary solution

$$\begin{aligned} \rho(\theta, \omega, t) &= \frac{1}{2\pi} \\ r(t) &= 0 \end{aligned} \tag{2.14}$$

corresponding to the *incoherent* state where all oscillators are drifting, with uniform probability distribution for the phases of the oscillators in the interval $[0, 2\pi]$.

For finite, nonzero values of the coupling constant K, we have other possible solutions: the *partially synchronized* states [6, 11, 12] for which $0 < r < 1$. The construction of these solutions starts from the following ansatz: the set of oscillators splits into a set of incoherent, drifting oscillators, and another set of oscillators, whose average phase ψ rotates with constant frequency Ω, so that r does not depend on time.

For the sake of simplicity let us change to a rotating frame with constant angular velocity Ω and define a new angular variable $\phi = \theta - \Omega t$, implying $\dot{\theta} = \dot{\phi} + \Omega$. Looking for solutions where $\dot{\phi}$, the instantaneous phase velocity of the oscillators in the rotating frame, is equal to zero, Eq.(2.12) yields

$$0 = \omega - \Omega - Kr\sin\phi. \tag{2.15}$$

The oscillators with $Kr \geqslant |\omega - \Omega|$ asymptotically approach a stable fixed point ϕ^* defined by

$$\sin\phi^* = \frac{\omega - \Omega}{Kr}, \qquad \phi^* \in \left[-\frac{\pi}{2}, \frac{\pi}{2}\right] \tag{2.16}$$

synchronized (it is easy to check that the other solution of Eq.(2.16) is an unstable fixed point.) If these oscillators approach a fixed point in the rotating frame $\psi(t) = \Omega t$ they are locked at frequency Ω in the original frame, defining a probability density

$$\rho(\theta, \omega, t) = \delta\left[\theta - \Omega t - \sin^{-1}\left(\frac{\omega}{Kr}\right)\right], \quad |\omega| \leqslant Kr \tag{2.17}$$

11

where δ is the Dirac-*delta* function. Note that $\rho(\theta, \omega, t) = \rho(\phi, \omega)$, so that Eq.(2.17) is stationary in the rotating frame.

On the other hand, oscillators with $|\omega| > Kr$ are drifting. Let us look for stationary solutions $\rho(\phi, \omega)$ in the rotating frame for the phase distribution of this second set of oscillators. Then $\rho(\phi, \omega)$ must be inversely proportional to the speed at ϕ

$$\rho(\phi, \omega) = \frac{C(\omega)}{|\omega - Kr \sin \phi|}, \quad |\omega| > Kr. \quad (2.18)$$

Then, for the partially synchronized states we arrived at the two branches of the solution: The locked one, with oscillators $|\omega| \leq Kr$ and the drifting one, with oscillators $|\omega| > Kr$.

$$\rho(\theta, \omega, t) = \begin{cases} \delta\left[\theta - \Omega t - \sin^{-1}\left(\frac{\omega}{Kr}\right)\right], & |\omega| \leq Kr \\ \\ \frac{C(\omega)}{|\omega - Kr \sin(\theta - \Omega t)|}, & |\omega| > Kr \end{cases} \quad (2.19)$$

where $C(\omega)$ is to be determined using the normalisation condition for $\rho(\theta, \omega, t)$, Eq.(2.5), yielding

$$C(\omega) = \frac{\sqrt{\omega^2 - (Kr)^2}}{2\pi}. \quad (2.20)$$

This construction will work provided that Eq.(2.6) with $\rho(\theta, \omega, t)$ given by Eq.(2.19) can be solved self-consistently for r and Ω.

2.1.2 Evaluation of the Order Parameter and Critical Coupling

Substituting the density ρ, given by Eq.(2.19) into Eq.(2.6) we get the condition

$$r = \int_0^{2\pi} \int_{-\infty}^{+\infty} e^{i(\theta - \Omega t)} \left(\delta\left[\theta - \Omega t - \sin^{-1}\left(\frac{\omega}{Kr}\right)\right] g(\omega) + \frac{C(\omega) g(\omega)}{|\omega - Kr \sin(\theta - \Omega t)|} \right) d\omega d\theta. \quad (2.21)$$

Spliting the contribution of the locked and drift oscillators as first and second term we get

$$\begin{aligned} r &= \int_0^{2\pi} \int_{|\omega| \leq Kr} e^{i(\theta - \Omega t)} \delta\left[\theta - \Omega t - \sin^{-1}\left(\frac{\omega}{Kr}\right)\right] g(\omega) d\omega d\theta + \\ &+ \int_0^{2\pi} \int_{|\omega| > Kr} e^{i(\theta - \Omega t)} \frac{C(\omega) g(\omega)}{|\omega - Kr \sin(\theta - \Omega t)|} d\omega d\theta. \end{aligned} \quad (2.22)$$

If we take $\Omega = \bar{\omega}$, the second term vanishes, since then $g(\omega) = g(-\omega)$, as we assumed in the beginning, and $\rho(\theta + \pi, -\omega) = \rho(\theta, \omega)$. So we get

$$r = \int_0^{2\pi} \int_{|\omega| \leq Kr} e^{i(\theta - \Omega t)} \delta\left[\theta - \Omega t - \sin^{-1}\left(\frac{\omega}{Kr}\right)\right] g(\omega) d\omega d\theta, \quad (2.23)$$

Developing the exponential yields

$$r = \int_0^{2\pi} \int_{|\omega| \leq Kr} \cos(\theta - \Omega t)\delta\left[\theta - \Omega t - \sin^{-1}\left(\frac{\omega}{Kr}\right)\right]g(\omega)d\omega d\theta +$$
$$+i \int_0^{2\pi} \int_{|\omega| \leq Kr} \sin(\theta - \Omega t)\delta\left[\theta - \Omega t - \sin^{-1}\left(\frac{\omega}{Kr}\right)\right]g(\omega)d\omega d\theta \qquad (2.24)$$

To be consistent with the initial construction of r as a real quantity the imaginary part of Eq.(2.24) must be zero, which we will verify now.

$$\int_0^{2\pi} \int_{|\omega| \leq Kr} \sin(\theta - \Omega t)\delta\left[\theta - \Omega t - \sin^{-1}\left(\frac{\omega}{Kr}\right)\right]g(\omega)d\omega d\theta =$$
$$= \int_{|\omega| \leq Kr} \sin\left[\sin^{-1}\left(\frac{\omega}{Kr}\right)\right]g(\omega)d\omega \qquad (2.25)$$

If we put $\zeta = \sin^{-1}\left(\frac{\omega}{Kr}\right)$, which implies $\frac{\omega}{Kr} = \sin\zeta$ or $\omega = Kr\sin\zeta$ with $\zeta \in [-\frac{\pi}{2}, \frac{\pi}{2}]$ we get

$$\frac{d\omega}{d\zeta} = Kr\cos\zeta. \qquad (2.26)$$

Changing the variable of integration in the right hand side of Eq.(2.25 from ω to ζ yields

$$\int_{-\frac{\pi}{2}}^{\frac{\pi}{2}} \sin\zeta g(Kr\sin\zeta)Kr\cos\zeta d\zeta$$

that is

$$Kr\int_{-\frac{\pi}{2}}^{\frac{\pi}{2}} \sin\zeta \cos\zeta g(Kr\sin\zeta)d\zeta \qquad (2.27)$$

Since we assumed $g(\omega)$ to be in the fixed frame unimodal and symmetric about its mean frequency $\bar{\omega} = \Omega$, $g(\omega) = g(-\omega)$ in the rotating frame and Eq.(2.27) is indeed zero.

Retaining only the real part of Eq.(2.24) we can resume the finding of the critical coupling and of an expression for r at the transition. Changing the order of integration in the real part of Eq.(2.24) yields

$$r = \int_{|\omega| \leq Kr} \int_0^{2\pi} \cos(\theta - \Omega t)\delta\left[\theta - \Omega t - \sin^{-1}\left(\frac{\omega}{Kr}\right)\right]g(\omega)d\theta d\omega, \qquad (2.28)$$

and performing the integral in θ we get

$$r = \int_{|\omega| \leq Kr} \cos\left[\sin^{-1}\left(\frac{\omega}{Kr}\right)\right]g(\omega)d\omega \qquad (2.29)$$

Now, if we put $\chi = \sin^{-1}\left(\frac{\omega}{Kr}\right)$, which implies $\frac{\omega}{Kr} = \sin\chi$ or $\omega = Kr\sin\chi$ with $\chi \in [-\frac{\pi}{2}, \frac{\pi}{2}]$ we get

$$\frac{d\omega}{d\chi} = Kr\cos\chi. \qquad (2.30)$$

13

Changing the variable of integration in Eq.(2.29) from ω to χ yields

$$r = \int_{-\frac{\pi}{2}}^{\frac{\pi}{2}} \cos\chi g(Kr\sin\chi)Kr\cos\chi d\chi$$

that is

$$r = Kr \int_{-\frac{\pi}{2}}^{\frac{\pi}{2}} \cos^2\chi g(Kr\sin\chi)d\chi \tag{2.31}$$

Along with the trivial solution $r = 0$ corresponding to completely unlocked oscillators we find a second branch of solutions corresponding to the partially synchronized ones

$$1 = K \int_{-\frac{\pi}{2}}^{\frac{\pi}{2}} \cos^2\chi g(Kr\sin\chi)d\chi \tag{2.32}$$

By setting $r = 0$ in Eq.(2.32) we find the value of $K = K_c$ of the coupling constant from which this partially synchronized branch bifurcates. In fact, for $r = 0$, Eq.(2.32) becomes

$$1 = K_c \int_{-\frac{\pi}{2}}^{\frac{\pi}{2}} \cos^2\chi g(0)d\chi$$

or

$$\frac{1}{g(0)} = K_c \int_{-\frac{\pi}{2}}^{\frac{\pi}{2}} \cos^2\chi d\chi,$$

implying

$$K_c = \frac{2}{\pi g(0)} \tag{2.33}$$

For the particular case of a Lorentzian density

$$g(\omega) = \frac{\gamma}{\pi(\gamma^2 + \omega^2)} \tag{2.34}$$

an explicit evaluation of the above integrals gives

$$r = \sqrt{1 - \frac{K_c}{K}}, \quad K > K_c = 2\gamma \tag{2.35}$$

For a general density distribution $g(\omega)$ we Taylor expand $g(Kr\sin\chi)$ in powers of Kr getting

$$g(0) + Kr\sin\chi g'(0) + \frac{(Kr)^2}{2}\sin^2\chi g''(0) + O(Kr)^2 \tag{2.36}$$

and substituting into Eq.(2.32) we obtain a scaling law for r

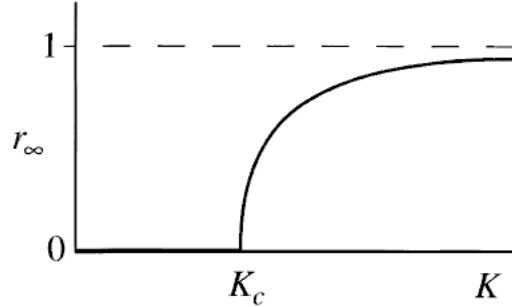$$r \sim \sqrt{\frac{(K - K_c)}{g''(0)}}. \tag{2.37}$$

14

Figure 2.2: Second order phase transition. With $K < K_c$ the real part of the order parameter is zero. At $K = K_c$ the order parameter bifurcate continuously, begin a partially synchronized state.

The radial part of the normal form in polar coordinates for the Hopf bifurcation [10] is given by

$$r = \sqrt{\frac{-d\mu}{a}} \tag{2.38}$$

where $d = \alpha'(0)$, $a = a(0)$ with $\mu = K - K_c$ in the normal form $\dot{r} = \alpha(\mu)r + ar^3$. If $g''(0) < 0$ as in the case of a Gaussian or Lorentzian distributions, we have a supercritical Hopf bifurcation.

Without coupling constant K all oscillators are free to move at their own frequency. Eventually, as K increases it reaches a critical value K_c above which some oscillators begin to synchronize, and where the effective coupling constant $Kr(t)$, as can be seen by Eq.(2.4), undergoes a positive feedback, being greater for a greater number of entrained oscillators.

At K_c we face a phenomenon similar to a second order phase transition with an order parameter given by Eq.(2.2). This link between statistical physics and dynamical systems showed to be very fruitful. As Kuramoto wrote [11]

> It is expected that the supercritical bifurcating solution is stable, and the subcritical one is unstable. Again, this fact appears to be difficult to prove. Physically, why the sign of $g''(0)$ determines the direction of branching of the non-zero solution may be qualitatively understood as follows. If g is concave at $\omega = \omega_0$, then the "nucleation" of synchronized oscillators, once initiated, will be speeded up due to the increasing number density of the oscillators just participating in the nucleation. As a result, the cluster growth will not be suppressed until its size reaches a fairly large value.

2.1.3 Stability of The Incoherent Solution

Here we will address briefly the stability problem of the incoherent solution expressed by Eq.(2.14). Although in recent years there have been major advances in understanding the stability of the partially locked [13] and locked [14] solutions, the global stability analysis of system has been made only for the case of a Lorentzian distribution of proper frequencies [15]-[16].

It's worth noting that the incoherent and the partially synchronized solutions are meaningful only in the thermodynamic limit, although for a finite number of oscillators we will see, in certain conditions, a behaviour similar to partially synchronized solution.

Lets consider a small perturbation away from the incoherent state

$$\rho(\theta, \omega, t) = \frac{1}{2\pi} + \varepsilon\eta(\theta, \omega, t), \quad \varepsilon \ll 1 \tag{2.39}$$

The normalization condition Eq.(2.5) implies that

$$\int_0^{2\pi} \eta(\theta, \omega, t) = 0, \tag{2.40}$$

and introducing the perturbed incoherent state Eq.(2.39) in the continuity equation (2.11) we get the evolution equation

$$\varepsilon\frac{\partial \eta}{\partial t} - \frac{\partial}{\partial \theta}\left[(\frac{1}{2\pi} + \varepsilon\eta)v\right] = 0 \tag{2.41}$$

We are interested in the lowest order in ε. Observing from Eq.(2.6) that $r(t)$ is $O(\varepsilon)$ and using Eq.(2.12) we get

$$r(t) = \varepsilon r_1(t) + O(\varepsilon^2) \tag{2.42}$$

where

$$r_1(t)e^{i\psi(t)} = \int_0^{2\pi} \int_{-\infty}^{+\infty} e^{i\theta(t)}\eta(\theta, \omega, t)g(\omega)d\omega d\theta. \tag{2.43}$$

From Eq.(2.12) we get $\frac{\partial v}{\partial \theta} = -\varepsilon K r_1(t)\cos(\psi(t) - \theta(t))$. At $O(\varepsilon)$ the evolution equation (2.41) becomes

$$\frac{\partial \eta(\theta, \omega, t)}{\partial t} - \omega\frac{\partial \eta(\theta, \omega, t)}{\partial \theta} + \frac{K}{2\pi}r_1(t)\cos(\psi(t) - \theta(t)) = 0. \tag{2.44}$$

Since $\eta(\theta, \omega, t)$ is real and 2π-periodic in θ we will seek solutions of Eq.(2.44) on the form

$$\eta(\theta, \omega, t) = c(\omega, t)e^{i\theta(t)} + c^*(\omega, t)e^{-i\theta(t)} + \eta^\perp(\theta, \omega, t) \tag{2.45}$$

Where $*$ denote complex conjugate and $\eta^\perp(\theta, \omega, t)$ contain all harmonics largest than the first.

16

Before we proceed let us show that the only contribution of η to the final term of Eq.(2.44) is throug $c(\omega, t)$ and his complex conjugate.

To see this note that $r_1(t)\cos(\psi(t)-\theta(t)) = Re\left[r_1(t)e^{i\psi(t)}e^{-i\theta(t)}\right]$. Substituting Eq.(2.45) into Eq.(2.43) yields

$$r_1(t)e^{i\psi(t)} = 2\pi \int_{-\infty}^{+\infty} c^*(\omega, t)g(\omega)d\omega \tag{2.46}$$

and

$$
\begin{aligned}
r_1(t)\cos(\psi(t) - \theta(t)) &= 2\pi Re\left[\left(\int_{-\infty}^{+\infty} c^*(\omega, t)g(\omega)d\omega\right)e^{-i\theta}\right] \\
&= \pi\left(\int_{-\infty}^{+\infty} c^*(\omega, t)g(\omega)d\omega\right)e^{i\theta} + c.c.
\end{aligned}
\tag{2.47}
$$

where c.c. denotes the complex conjugate of the preceding term. Now is clear that the last term of Eq.(2.44) depends only on $c(\omega, t)$ and its complex conjugate.

Inserting Eq.(2.45) and Eq.(2.47) into Eq.(2.44) and equating the coefficients of $e^{i\theta(t)}$ on both sides of the resulting equation we get the evolution equation for the fundamental mode $c(\omega, t)$

$$\frac{\partial c(\omega, t)}{\partial t} = -i\omega c(\omega, t) + \frac{K}{2}\int_{-\infty}^{+\infty} c(t, \nu)g(\nu)d\nu. \tag{2.48}$$

The right hand side of Eq.(2.48) defines a linear operator A which has both a discrete and a continuous spectrum. The discrete spectrum is given by solutions to

$$1 = \frac{K}{2}\int_{-\infty}^{\infty} \frac{g(\omega)}{\lambda + i\omega}d\omega \tag{2.49}$$

For $g(\omega)$ even and nonincreasing in $[0, +\infty]$ there is either no discrete spectrum (for $K \leq K_c$), or a unique and positive real discrete spectrum which tends to 0 as $K \to K_c^+$.

Thus the incoherent solution is always linearly *neutrally stable*.

2.2   Chimeras

When we talk about chimeras we mean anything that seems fantastic or composed of incongruous parts. In Greek mythology, a chimera was a fire-breathing monster having a lion's head, a goat's body, and a serpent's tail. A mathematical chimera - the one that interests us - is an array of identical oscillators that split into two domains: one coherent, or synchronized, and the other incoherent.

This splitting cannot be ascribed to the inhomogeneity of the oscillators themselves as in the previous sections where each oscillator had its own frequency [17]. Kuramoto first reported chimeras (the name was given by himself) back in 2003 when studying arrays of

identical limit cycle oscillators that were coupled nonlocally [18]. In fact, most of the work on coupled oscillators until a few years ago has focused either on local (nearest neighbours) or all-to-all (global) coupling. So, from a theoretical point of view, nonlocal coupling was the natural path to follow in the research. On the other and, nonlocal coupling arises in diverse systems throughout physics, chemistry and biology [19].

The simplest system that supports a chimera state, a continuous ring of coupled phase oscillators [17, 18, 19] can be described by

$$\dot{\theta}(x,t) = \omega - \int_{-\pi}^{\pi} G(x-x')\sin[\theta(x,t) - \theta(x',t) + \alpha]dx' \tag{2.50}$$

with the usual notation. The frequency ω plays no role in the dynamics, in the sense that one can set $\omega = 0$ by shifting θ by the amount ωt, and the kernel $G(x-x')$ provides nonlocal coupling between the oscillators and it is assumed to be even, non-negative, decreasing with the separation $|x - x'|$ along the ring, and normalised to have unit integral.
We proceed by using a generalisation of Kuramoto's self-consistency method [19]. Let Ω denote the angular frequency of the rotating frame in which the dynamics become as simple as possible and let

$$\phi(x,t) = \theta(x,t) - \Omega t \tag{2.51}$$

denote the phase of an oscillator relative to this frame. So $\dot{\phi}(x,t) = \dot{\theta}(x,t) - \Omega$. Knowing this Eq.(2.50) can be rewritten in terms of the new phase ϕ

$$\dot{\phi}(x,t) = \omega - \Omega - \int_{-\pi}^{\pi} G(x-x')\sin[\phi(x,t) - \phi(x,t) + \alpha]dx'. \tag{2.52}$$

We can now introduce a time and space dependent complex-valued order parameter

$$R(x,t)e^{i\Phi(x,t)} = \int_{-\pi}^{\pi} G(x-x')e^{i\phi(x',t)}dx' \tag{2.53}$$

Multiplying both sides of the order parameter by $e^{-i(\alpha+\phi(x,t))}$ and equating imaginary parts

$$R(x,t)\sin(\phi(x,t) - \Phi(x,t) + \alpha) = \int_{-\pi}^{\pi} G(x-x')\sin[\phi(x,t) - \phi(x',t) + \alpha]dx'. \tag{2.54}$$

With Eq.(2.54) we can rewrite the governing equation (2.52) as

$$\dot{\phi}(x,t) = \omega - \Omega - R(x,t)\sin[\phi(x,t) - \Phi(x,t) + \alpha] \tag{2.55}$$

and we can see that equation (2.55) is formally equivalent to equation (2.4) which suggests that we can proceed using the self-consistency arguments of mean field theory, although the system is not globally coupled.

18

Now we pay attention to stationary solutions, in which R and Φ are functions only of the space variable. The oscillators with $R(x) \geq |\omega - \Omega|$ asymptotically approach a stable fixed point $\phi^*(x)$, defined implicitly by

$$\frac{\omega - \Omega}{R(x)} = \sin[\phi^*(x) - \Phi(x) + \alpha] \tag{2.56}$$

and if these oscillators approach a fixed point in the rotating frame (see Eq.(2.51) for the definition of ϕ), they are locked at frequency Ω in the original frame. And the oscillators with $R(x) < |\omega - \Omega|$ are the ones that are drifting.

As we are working with stationary solutions, these oscillators must distribute themselves according to a stationary probability density $\rho(\phi, x)$. This requires that $\rho(\phi, x)$ be inversely proportional to the speed at ϕ

$$\rho(\phi, x) = \frac{C(x)}{|\omega - \Omega - R(x)\sin[\phi(x) - \Phi(x) + \alpha]|}. \tag{2.57}$$

With the normalisation constant chosen such that that $\int_{-\pi}^{\pi} \rho(\phi, x)d\phi = 1$, Eq.(2.57) becomes

$$\rho(\phi, x) = \frac{\sqrt{(\omega - \Omega)^2 - R^2(x)}}{2\pi|\omega - \Omega - R(x)\sin[\phi(x) - \Phi(x) + \alpha]|}. \tag{2.58}$$

We must stress that the resulting motion of both the locked and drifting oscillators must be consistent with the assumed stationarity for $R(x)$ and $\Phi(x)$.

To calculate the contribution that both locked and drifting oscillators make to the order parameter, Eq.(2.53), we see that

$$\sin(\phi(x) - \Phi(x) + \alpha) = \frac{\omega - \Omega}{R(x)}.$$

and using the trigonometric identity $\sin^2\phi + \cos^2\phi = 1$ we get

$$\cos(\phi(x) - \Phi(x) + \alpha) = \pm\frac{\sqrt{R(x)^2 - (\omega - \Omega)^2}}{R(x)} \tag{2.59}$$

for any solution $\phi(x)$ of Eq.(2.56).

To find out the contribution of the locked oscillators to the order parameter Eq.(2.53) we can use the trigonometric identity $\cos\phi = \sin(\frac{\pi}{2} - \phi)$ to see that in Eq.(2.59) the stable fixed point of Eq. (2.55) corresponds to the plus sign. Then

$$e^{i(\phi^*(x) - \Phi(x) + \alpha)} = \frac{\sqrt{R^2(x) - \delta^2} + i\delta}{R(x)}, \tag{2.60}$$

where $\delta = (\omega - \Omega)$, and so the contribution of the locked oscillators to the order parameter (2.53) and taking into account the assumed stationarity of $R(x)$ and $\Phi(x)$, becomes

19

$$R(x)e^{i\Phi(x)} = e^{-i\alpha} \int_{D_1} G(x-x')e^{i\Phi(x')} \frac{\sqrt{R^2(x') - \delta^2} + i\delta}{R(x')} dx' \qquad (2.61)$$

where $D_1 = \{x' : R(x') \geq |\delta|\}$ and we have subtracted α and Φ from Eq.(2.60) to maintain the identity.

The contribution of the drifting oscillators can be calculated [18, 19] replacing $e^{i\phi(x')}$ in Eq.(2.53) by its statistical average

$$R(x)e^{i\Phi(x)} = \int_{D_2} G(x-x') \int_{-\pi}^{\pi} e^{i\phi} \rho(\phi, x')) d\phi dx'. \qquad (2.62)$$

Where $D_2 = \{x' : R(x') < |\delta|\}$. Substituting Eq.(2.58) for ρ into Eq.(2.62) and evaluating the integral yields

$$\int_{-\pi}^{\pi} e^{i\phi} \frac{\sqrt{(\omega - \Omega)^2 - R^2(x')}}{2\pi |\omega - \Omega - R(x') \sin[\phi - \Phi(x') + \alpha]|} d\phi = \frac{i}{R(x')}(\delta - \sqrt{\delta^2 - R^2(x')}) \qquad (2.63)$$

Therefore the contribution of the drifting oscillators to the order parameter Eq.(2.53)becomes

$$R(x)e^{i\Phi(x)} = \int_{D_2} G(x-x') \frac{\sqrt{R^2(x') - \delta^2} + i\delta}{R(x')} dx' \qquad (2.64)$$

Thus we obtained

$$R(x)e^{i\Phi(x)} = \begin{cases} e^{-i\alpha} \int_{D_1} G(x-x')e^{i\Phi(x')} \frac{\sqrt{R^2(x') - \delta^2} + i\delta}{R(x')} dx', & \text{for locked oscillators} \\ \\ \int_{D_2} G(x-x') \frac{\sqrt{R^2(x') - \delta^2} + i\delta}{R(x')} dx', & \text{for drift oscillators} \end{cases}$$

$$(2.65)$$

Chapter 3

Kuramoto Model With a Finite Number of Oscillators

3.1 Existence and Stability of Solutions

From now on we will focus on systems with a finite number of oscillators. The consideration of the limit $N \to \infty$ allows for several conclusions to be drawn, and this is realistic for a great many number of phenomena. However, and since 2004 [29], a great deal of attention has been devoted to finite populations of oscillators both in theoretical and computational aspects. Because the analysis of the model in the thermodynamic limit cannot simply be transposed to the case with a finite number of oscillators, and analytical results are hard to obtain, most research focuses on simulations [30].

We will need a more accurate terminology. Following [29] we reserve the term *phase locking* to a state where the phase differences between all the oscillators are constant, *full synchronization* to a state defined as phase locking with phase differences equal to zero and *partial entrainment* to a state where we have at least two oscillators with a constant phase difference.

We introduce the phase differences ϕ_j as

$$\phi_i(t) = \theta_i(t) - \theta_1(t), \quad i = 1, ..., N \tag{3.1}$$

and we can rewrite Eq.(2.4) as

$$\begin{cases} \dot{\theta}_1 &= \omega_1 + Kr(t)\sin(\psi(t) - \theta_1(t) \\ \dot{\phi}_i &= \omega_i - \omega_1 + Kr(t)[\sin(\psi(t) - \phi_i(t) - \theta_1(t)) - \sin(\psi(t) - \theta_1(t)], \quad i = 2, ..., N \end{cases} \tag{3.2}$$

In a state of phase locking, which according to the definition corresponds to $\phi_i(t)$ being a constant, the order parameter Eq.(2.2) can be written as

$$\left(\frac{1}{N}\sum_{j=1}^{N}e^{i\phi_j}\right)e^{i\theta_1(t)} \tag{3.3}$$

From now on we will denote $\frac{1}{N}\sum_{j=1}^{N}e^{i\phi_j}$ as $r_\ell e^{i\alpha}$. With this new notation slightly adapted from [29], we can write the order parameter Eq.(2.2) in the phase locking situation as

$$r(t)e^{i\psi(t)} = r_\ell e^{i(\alpha+\theta_1(t))} \tag{3.4}$$

From Eqs.(3.2) and (3.4), a phase locking solution satisfy

$$\begin{cases} \dot{\theta}_1 & = \omega_1 + Kr_\ell\sin(\alpha) \\ 0 & = \omega_i - \omega_1 + Kr_\ell\sin(\alpha - \phi_i) - Kr_\ell\sin(\alpha), \quad i = 2, ..., N \end{cases} \tag{3.5}$$

If we sum up all $N-1$ equations in (3.5) we will get

$$\omega_1 + Kr_\ell\sin(\alpha) = \frac{1}{N}\sum_{j=1}^{N}\omega_j + \frac{1}{N}Kr_\ell\sum_{j=1}^{N}\sin(\alpha - \phi_j) \tag{3.6}$$

and this yields

$$\dot{\theta}_1(t) = \frac{1}{N}\sum_{j=1}^{N}\omega_j + \frac{1}{N}Kr_\ell\sum_{j=1}^{N}\sin(\alpha - \phi_j) \tag{3.7}$$

If we take in to account our notation for $r_\ell e^{i\alpha}$ and the fact that, by definition $r_\ell \in [0, 1]$, then the following definition holds

$$r_\ell = \frac{1}{N}\sum_{j=1}^{N}\cos(\phi_j - \alpha) \tag{3.8}$$

If we notice that $\sum_{j=1}^{N}\sin(\alpha - \phi_j) = Im\left(\sum_{j=1}^{N}e^{i\alpha}e^{-i\phi_j}\right)$ and that $\sum_{j=1}^{N}\cos(\phi_j - \alpha) = Re\left(\sum_{j=1}^{N}e^{i\phi_j}e^{-i\alpha}\right)$ and using the notation previously introduced of expressing $\sum_{j=1}^{N}e^{i\phi_j}$ as $e^{i\alpha}$, we get $Im\left(\sum_{j=1}^{N}e^{i\alpha}e^{-i\phi_j}\right) = Im[1] = 0$ and $Re\left(\sum_{j=1}^{N}e^{i\phi_j}e^{-i\alpha}\right) = 1$.

Eq.(3.7)then yields

$$\dot{\theta}_1(t) = \frac{1}{N}\sum_{j=1}^{N}\omega_j. \tag{3.9}$$

Defining a new quantity, the *mean natural frequency*, ϖ as

$$\varpi = \frac{1}{N} \sum_{j=1}^{N} \omega_j \tag{3.10}$$

we can write the phase $\psi(t)$ of the complex order parameter Eq.(2.2), in the case of phase locking as

$$\psi(t) = \theta_1(t) + \alpha, \quad \Rightarrow \quad \psi(t) = \varpi t + \beta \tag{3.11}$$

with $\beta = \alpha + \theta_1(0)$.

So, in phase locking solutions all oscillators have a phase velocity equal to the mean natural frequency, which is a result that we could guess.

3.1.1 Conditions For The Existence of Phase Locking Solutions

Substituting Eq.(3.9) in Eq.(3.5) yields

$$0 = \omega_i - \varpi + K r_\ell \sin(\alpha - \phi_i), \quad i = 1, ..., N \tag{3.12}$$

Defining a new quantity $\delta_i = \omega_i - \varpi$, phase locking solutions satisfy

$$\sin(\phi_i - \alpha) = \frac{\delta_i}{K r_\ell}, \quad i = 1, ..., N \tag{3.13}$$

which yields a solution if and only if

$$K r_\ell \geq |\delta_i|, \quad i = 1, ..., N \tag{3.14}$$

Using the trigonometric identity $\sin^2(x) + \cos^2(x) = 1$ and Eqs.(3.8) and (3.13) we get a set of self-consistent equations in r_ℓ

$$r_\ell = \frac{1}{N} \sum_{j=1}^{N} \pm \sqrt{1 - \left(\frac{\delta_j}{K r_\ell}\right)^2} \tag{3.15}$$

We arrived at sufficient and necessary conditions for the existence of phase locking solutions: A solution $r_\ell(K)$ of Eq.(3.15) is a phase locking solution if and only if Eq.(3.14) is satisfied. Phase locking solutions of Eq.(3.15), (K, r_ℓ), are only possible for K greater than a threshold value K_c.

We can see this in a straightforward way looking to Eq.(3.15). The left hand side must be in $[0, 1]$, so the right hand side must have values in the same interval. Since Eq.(3.14) must allways hold in locking condition, and for given δ_j, r_ℓ and N, we have a threshold K_c above which the right hand side of Eq.(3.15) is between $[0, 1]$.

Other outcome that results from Eq.(3.13), somehow residual but interesting enough, is that in the phase locking situation, a great δ_i implies a great ϕ_i: The phase difference to oscillator 1 increases with the oscillator proper frequency.

3.1.2 Stability of the phase locking solution

Lets consider N oscillators described by Eq.(2.1). Substituting $\theta_i(t)$ by $\theta_i^*(t) + \varpi t$ yields

$$\dot{\theta}_i^* = \delta_i + \frac{K}{N} \sum_{j=1}^{N} \sin(\theta_j^* - \theta_i^*), \quad i = 1, ..., N \tag{3.16}$$

where $\delta_i = \omega_i - \varpi$, $\sum_{i=1}^{N} \delta_i = 0$, $\theta_i = \theta_i^* + \varpi t$ and we define $\theta^* = [\theta_1^* \cdots \theta_N^*]^T$ and remember that for a phase locking solution $\dot{\theta}_i(t) = \varpi$, or, in the new coordinates $\dot{\theta}_i^*(t) = 0$. First we must note that the system of equations (3.16) is invariant under translations.

$$\theta^* \to \theta^* + \alpha[1 \cdots 1]^T, \quad \text{for any} \quad \alpha \in \Re \tag{3.17}$$

So, each equilibrium point of 3.16 belongs to a curve of equilibrium points, all of them representing the same phase locking solution.

In [29] after the linearization of Eq.(3.16) is shown that the Jacobian of the linearization has a eigenvalue zero. The computation of the Jacobian yields

$$J = \frac{K}{N}(A + bb^T + cc^T) \tag{3.18}$$

with

$$
\begin{cases}
A &= -\mathrm{diag}(a_1, \cdots, a_N) \quad \text{with} \quad a_i = \pm N r_\ell \sqrt{1 - \left(\frac{\delta_i}{K r_\ell}\right)^2} \\[2mm]
b &= \left[\pm\sqrt{1 - \left(\frac{\delta_1}{K r_\ell}\right)^2} \cdots \pm \sqrt{1 - \left(\frac{\delta_N}{K r_\ell}\right)^2}\right]^T \in \Re^N \\[2mm]
c &= \left[\frac{\delta_1}{K r_\ell} \cdots \frac{\delta_N}{K r_\ell}\right]^T \in \Re^N
\end{cases}
\tag{3.19}
$$

Then in [29] they proceed to consider phase locking solutions with $\frac{|\delta_i|}{K r_\ell} < 1$ and show that phase locking solutions satisfying Eq.(3.15) with at least one minus sign are locally unstable. Finally the analysis is restricted to Eq.(3.15) with only positive signs and the following necessary and sufficient condition for stability is established:

$$\sum_{j=1}^{N} \frac{1 - 2\left(\frac{\delta_j}{K r_\ell}\right)^2}{\sqrt{1 - \left(\frac{\delta_j}{K r_\ell}\right)^2}} > 0 \tag{3.20}$$

24

Chapter 4

Finite number of oscillators with structured coupling

4.1 Synchronization in complex networks and known results in regular topologies

To the extent of our knowledge, most of the work in the study of a finite number of oscillators are found to be on all-to-all coupling, small-world and scale-free networks ([30], and references therein).

Since the seminal works of Watts and Strogatz [20, 21] and Barabási and Albert [22] lot of research has been done on networks shown small-world and scale-free properties. These networks resembles a wide range of natural phenomena or artificial constructions. From World-Wide-Web to epidemic spreading, the study of these complex networks showed to be a fruitfull path. An important issue concerning these networks is the interplay between structure and dynamics, in which the study of synchronization play an important role [23].

In a series of papers, Ermentrout *et. al.* [24, 25, 26, 27], done a extensively work on chains of weakly coupled oscillators with nearest neighbouring coupling, except in [27] where was introduced couplings beyond nearest neighbours.

To the best of our knowledge,their work, motivated by some undulate phenomena in mammalian small intestine, was the first serious work that deal with a finite number of oscillators and nearest-neighbour coupling and that could be partially integrated in Kuramoto model framework. They never mention Kuramoto's work because they couldn't do so: Kuramoto work [11] appear in the same year of the first paper.

Recently we have the work of A. Pikovsky and P. Rosenau [28] that intend to bridge two fields in nonlinear physics: synchrony and solitons and, using a ring as the topology of oscillators, a feature that we also make use, restrict their attention to dispersive coupling. Let us briefly use some results and techniques that appear in [24] with our terminology.

Lets consider a chain of $N+1$ phase coupled limit cycle oscillators with small coupling.

With the usual notation we get the set of equations

$$\dot{\theta}_1 = \omega_1 + K \sin(\phi_1) + O(K^2)$$
$$\dot{\phi}_i = K[\delta_i + \sin(\phi_{i+1}) + \sin(\phi_{i-1}) - 2\sin(\phi_i)] + O(K^2), \qquad i = 1, ..., N \qquad (4.1)$$

with the boundary conditions $\sin(\phi_0) = 0$ and $\sin(\phi_{N+1}) = 0$. To lowest order in K the equations for $\dot{\phi}_i$ are independent of θ_1. Letting $\tau = Kt$ we get $\overset{\bullet}{\phi} \equiv \frac{d\phi}{d\tau} = \frac{1}{K}\dot{\phi}$ and so the Eq.(4.1) for ϕ_i becomes

$$\overset{\bullet}{\vec{\phi}} = \vec{\delta} + \mathbf{\vec{G}}\,\mathbf{\vec{B}} \qquad (4.2)$$

where $\vec{\phi} = (\phi_1, ..., \phi_N)^T$, $\vec{\delta} = (\delta_1, ..., \delta_N)^T$, $\mathbf{\vec{B}} = (\sin(\phi_1), ..., \sin(\phi_N))^T$, and $\mathbf{\vec{G}}$ is the matrix with components $G_{ii} = -2$ and $G_{i+1,i} = G_{i,i+1} = 1$.

As we will see this resembles ours own approach, although this one is not useful to us since it is missing the boundary conditions..

4.2   Motivation for our choices and first analytical results

Here we work extensively with Gaussian distributions. Both in natural sciences and in social phenomena [31], a Gaussian distribution is vastly found to be the distribution that, within an approximation as good as you want gives the frequency of an ensemble of self sustained oscillators taken randomly from the entire population.

Moreover we set on 30 oscillators in this work. Our interest on a finite number of self-sustained oscillators was encouraged by the fact that, as much as we know, a great deal of work was done with two, three, four or even five oscillators (see [32, 33] and references therein). However these works were made to the intent of study the process of synchronization or desynchronization itself and not to present and study the phase behaviour and its relation, if we have one at all, with the proper frequencies of oscillators. On the other hand we want to surpass the limitation of a number of oscillators near to two or three, but not going to a number that could be only worked by statistical tools.

We choose a ring as the topology displayed by the oscillators. Since the works with a finite number of oscillators are residual when compared to that with an infinite number of oscillators, and even more residual if the coupling is nearest-neighbouring and not all-to-all, the ring is the simpler topology to work with.

Lets consider a ring with N oscillators. Writing down the governing equations yields

$$\dot{\theta}_i = \omega_i + K[\sin(\theta_{i+1} - \theta_i) + \sin(\theta_{i-1} - \theta_i))], \qquad i = 1, ..., N \qquad (4.3)$$

with boundary values conditions $\theta_{N+1} = \theta_1$ and $\theta_0 = \theta_N$. With the usual notation $\phi_i = \theta_{i+1} - \theta_i$ and $\delta_i = \omega_{i+1} - \omega_i$ with $i = 1, ..., N$ we get

$$\begin{cases} \dot{\phi}_i = \delta_i + K[\sin(\phi_{i+1}) + \sin(\phi_{i-1}) - 2\sin(\phi_i))], & i = 1, ..., N \\ \sum_{i=1}^{N} \phi_i = 0 \,(\mathrm{mod}\,2\pi) \\ \phi_{N+1} = \phi_1 \end{cases} \qquad (4.4)$$

These are the set of equations describing the evolution of ϕ with time in a ring of N oscillators.

To get insight in our system behaviour we will briefly see the discrete and linear limit and the continuous one. In the limit of small ϕ_i for which $\sin(x) \simeq x$ we get a set of linear equations describing the system in the linear and discrete limit

$$\begin{cases} \dot{\phi}_i = \delta_i + K(\phi_{i+1} + \phi_{i-1} - 2\phi_i), & i = 1, ..., N \\ \sum_{i=1}^{N} \phi_i = 0 \,(\mathrm{mod}\,2\pi) \\ \phi_{N+1} = \phi_1 \end{cases} \qquad (4.5)$$

and we can seek the fixed points of Eq.(4.5) solving

$$\mathbf{A}\vec{\phi} = \vec{\delta}, \qquad \vec{\phi} = [\phi_1, ..., \phi_N]^T \quad \text{and} \quad \vec{\delta} = [\delta_1, ...\delta_N]^T \qquad (4.6)$$

being $\mathbf{A}$ the laplacian of a ring. The linearised equation is the discrete laplacian, or, put in another way, is simply the laplacian operator applied to the ensemble of ϕ_i which in operatorial form is expressed by the Eq.(4.6).

Now we easily see that $\mathbf{A}\vec{\phi} = \vec{\delta}$ has the form of a eigenvalue equation $\mathbf{A}\vec{\nu} = a_i\vec{\nu}$ where $a_i\vec{\nu} = \vec{\delta}$ and $\vec{\nu} = \vec{\phi}$. To each input $\vec{\delta}$ we get a $\vec{\phi}$ and so in the linear and discrete approximation each $\vec{\phi}$ is a eigenvector of the laplacian and each $\vec{\delta}$ can be decomposed in $a_i\vec{\delta'}$ where a_i is an eigenvalue of the laplacian and $\vec{\delta'}$ a eigenvector.

The laplacian for the ring graph on N vertices (oscillators) has the eigenvectors [35]

$$(x(u), y(u)) = \left(\sin\left(\frac{2\pi K u}{N}\right), \cos\left(\frac{2\pi K u}{N}\right) \right), \quad \text{for } 0 \leq K \leq \frac{N}{2} \qquad (4.7)$$

with eigenvalues $2 - 2\cos(\frac{2\pi K}{N})$.

In the case of an odd ring, the eigenvector associated with the larger eigenvalue have the structure $(+a, -b, +c, -c, +b, -a, 0)$ and $(+a, -a, +a, -a, +a, -a)$ for even rings. And the eigenvector associated with the lowest eigenvalue other than zero is always of the general form $(+a, +b, +c, -c, -b, -a, 0)$ for the odd ring and $(+a, -a, -b, -a, +a, b)$ for the even one, where $a, b \in R$.

We can see from this that the largest eigenvalue has associated eigenvector with a greater asymmetry than the lowest one, In fact, as we will see, in a convenient space we can, to a certain extent, predict what phase measure (a measure in that space) we will get for a given proper frequency distribution in the ring.

On the continuous limit we get, form Eq.(4.5), the non homogeneous diffusion equation

$$\dot{\phi} = \delta + K \frac{\partial^2 \phi}{\partial \phi^2} \tag{4.8}$$

That the phase difference ϕ in a chain of oscillators in the continuum limit is described by a non homogeneous diffusion equation is well known in the literature, e.g.[25].

Before we proceed by this way we'll see some features of a system of 30 oscillators with a nearest neighbouring coupling.

4.2.1 Parameters of integration and graphics display

We use the free software XPPAUT [34] to integrate Eq.(2.1) using a second order Runge-Kutta with a time step of 0.05 and a time of integration of 200, getting 4000 steps. We could see in fig.(4.1) that the network quickly converge to its final phase distributions.
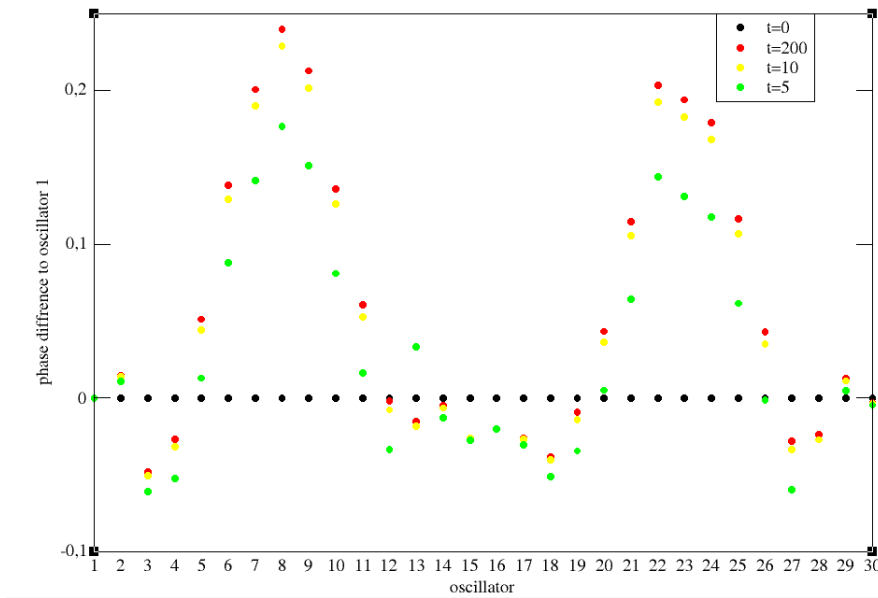
Figure 4.1: *Ring in which each oscillator is coupled to its nearest-neighbour and with the three frontal oscillators. Integration of Eq.2.1 with 30 oscillators and a Gaussian distribution of frequencies $N(2, 0.1)$. We see a rapid convergence to the final distribution of the phases.*

Each oscillator get its frequency from a Gaussian distribution of mean 2 and variance 0.1. As is well known the mean have no role in our system because we can always shift it

28

to a standard mean. The variance, and the coupling constant K on the other hand must be carefully chosen.

The oscillators are to be similar, that is, with a low dispersion of proper frequency. As we increase the variance, the synchrony is easily lost. In fig.(4.2) we increase the variance in a controled way to each oscillator in a known distribution. We can see that the final phase pattern become much more "loose", e.g., the phase difference to oscillator 1 increase rapidly and we become to the edge of synchrony, which eventually could be lost if we increase a little more the variance. We can also lost synchrony for a given topology if we decrease the coupling strength bellow its critical value. In fig.(4.3) we decrease K in such a way that synchrony is lost.
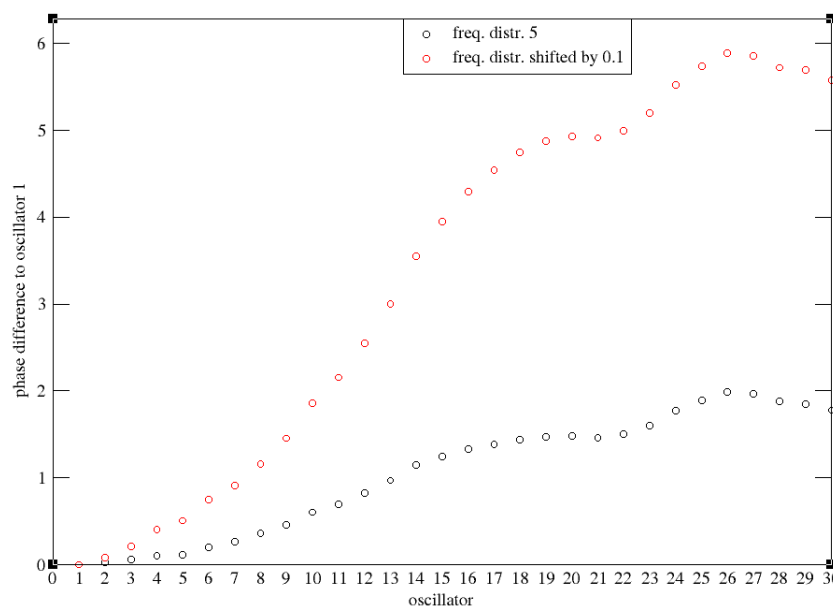
Figure 4.2: *Chain with nearest-neighbour coupling. Integration of Eq.2.1 with* 30 *oscillators and a Gaussian distribution of frequencies* $N(2, 0.1)$. *Then we shift each frequency by* 0.1 *and synchrony is almost lost.*

So, to the sake of simplicity and uniformity in the analysis of the results we set on the same distribution $N(2, 0.1)$. In some cases we are not interested on which frequency is assigned to each oscillator, and we do not refer the attribution of frequencies. However, as the work proceed we found necessary to see what frequencies are assigned to each oscillator, and we make it explicit.

Following [29] we plot the relative phase of each oscillator to oscillator 1. As we have a finite number of oscillators, we can always order them and label one of them as the first. As we saw in chapter 3 theoretical analysis also followed this procedure.
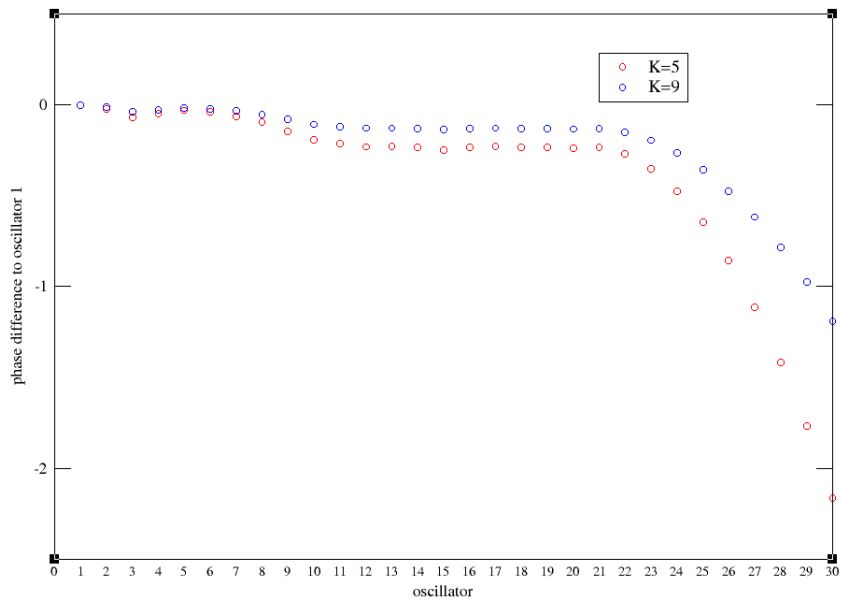
Figure 4.3: *Two chains with unidirectionally coupled oscillators coupled by oscillators* 14 *and* 15, *the heads of each chain. Integration of Eq.2.1 with* 30 *oscillators with frequency distribution* $N(2, 0.1)$.

A last remark on the interpretation of graphics. Fig.(4.4) show a static wave-like phase distribution. In fact we always must bear in mind that the plot is a "picture" on phase distribution after 4000 steps of integration, with the certainty, e.g. Fig.(4.1), that the system rapidly converge to its final phase distribution. What we see is a phase difference with respect to the what we label as first oscillator.

4.3   First numerical results and their analysis

We must stress that what we see is a static phase distribution relative to oscillator labelled with number 1. In a ring this procedure, though useful, is completely arbitrary. So we must try to see the system in its dynamics and not as a static one.

The coupling constant K is a key parameter in the Kuramoto model. She transform an ensemble of independent limit cycles oscillators into a new system weakly coupled that eventually evolve to a new state: synchrony. We are able to see how K affect phases distribution for the same distribution in Fig.(4.4).

As K increase the phase difference to oscillator 1 become increasingly small. This is what we might expect for K account for the coupling strength between a system of
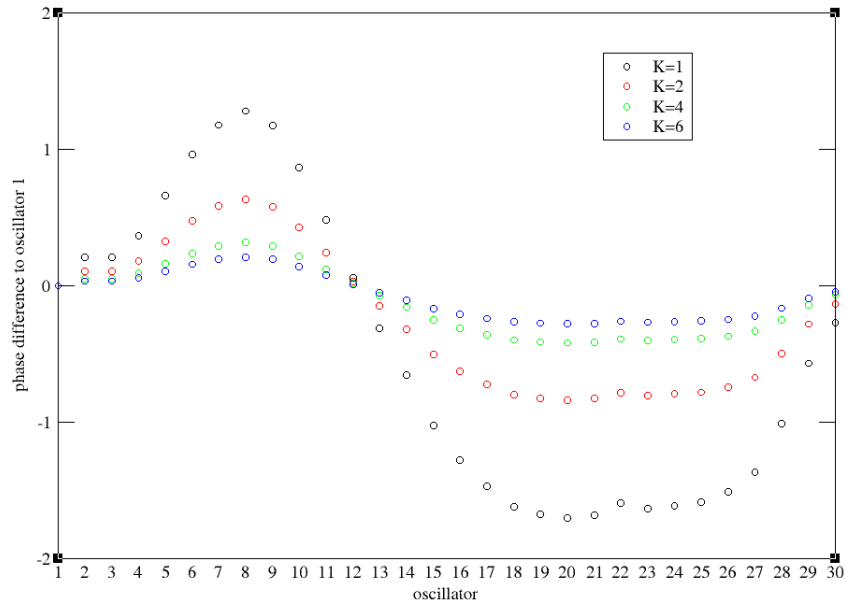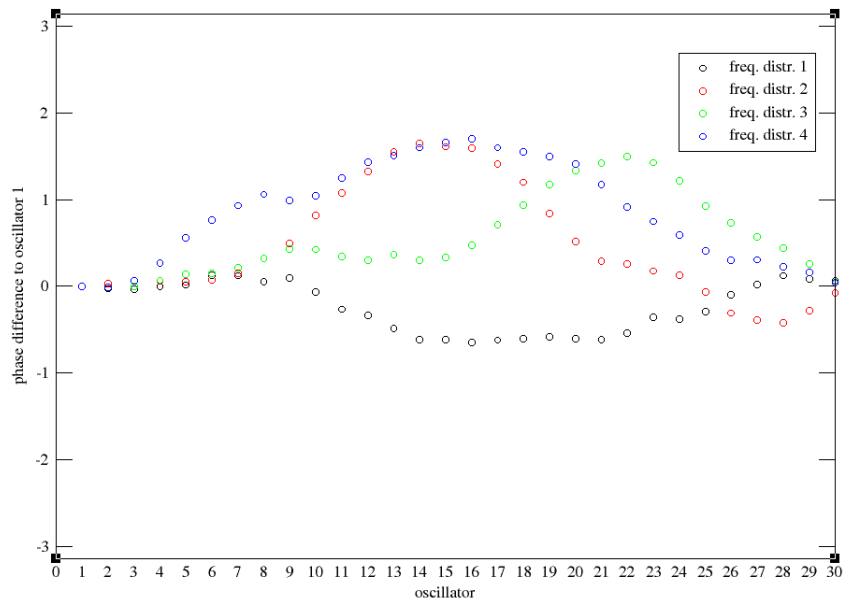
Figure 4.4: *Ring with nearest-neighbour coupling. Integration of Eq.2.1 with* 30 *oscillators. Same frequency distribution for four different coupling constant. As K increase the phase difference to the reference oscillator become lesser and lesser.*

oscillators that without K would behave as independent systems.

Frequency distribution is other parameter that determines the phase distribution. Each oscillator have its proper frequency that is picked up from a Normal distribution of given mean and variance.

We can infer from our integrations that for a different frequency distribution we have a completely different phase portrait. The phase relationship of oscillators with each others depends entirely, for fixed K, of the assignment of proper frequencies to the oscillators with Fig.(4.5) being an example. This dependence of the final phase distribution with the particular assignment of a frequency to a oscillator is also stressed when we permute some frequencies in a given frequency distribution.

In Fig. (4.6) we use some given frequency distribution and then we permute the frequency assigned to oscillator 3 to that of the oscillator 21 (red dots), and then we add another permutation by assigning to oscillator 18 the frequency of the oscillator 3. Even with only one permutation we obtain a completely different phase portrait.

Figure 4.5: *Ring with nearest-neighbour coupling. Integration of Eq.2.1 with* 30 *oscillators. Same frequency distribution for four different coupling constant. As K increase the phase difference to the reference oscillator become lesser and lesser.*
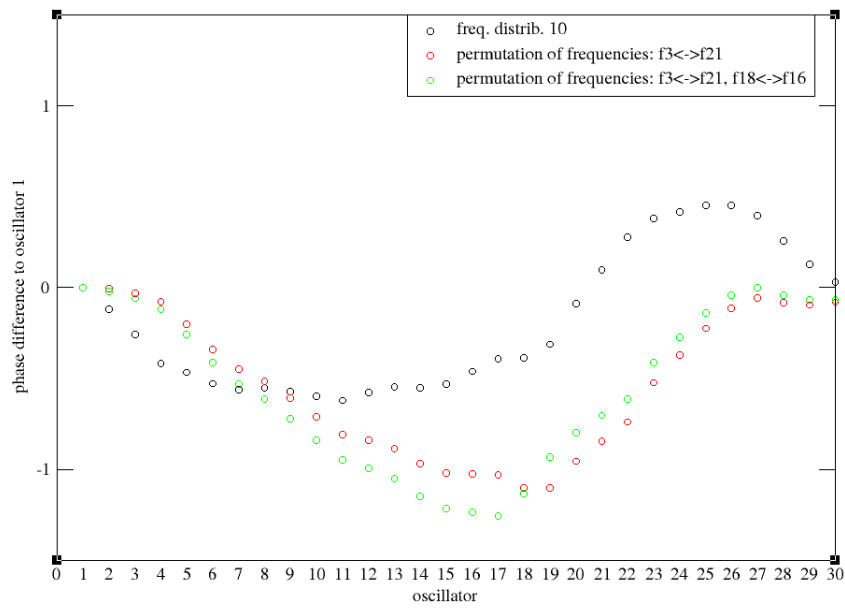
Figure 4.6: *Ring with nearest-neighbour coupling. Integration of Eq.(2.1) with* 30 *oscillators using the same coupling constant with different frequency distributions..*

4.3.1 Analitical results and insights from numerical integrations

The role of eigenvectors in describing our system

Our approach to the problem gained by the numerical insights take us to use the stable fixed points obtained by solving Eq.(4.6) as guesses to cubic approximation of the sine function, which in turn we use as guesses to the full sine version of Eq.(4.6) which is:

$$\begin{cases} 0 = \delta_i + K[\sin(\phi_{i+1}) + \sin(\phi_{i-1}) - 2\sin\phi_i], \quad i = 1, ..., N \\ \sum_{i=1}^{N} \phi_i = 0 \,(\mathrm{mod}\,2\pi) \\ \phi_{N+1} = \phi_1 \end{cases} \tag{4.9}$$

We choose as a space to make sense of the behaviour of our system the two dimensional space formed by $V1 = \sqrt{\sum_{i=1}^{N} \delta_i^2}$ in abscissa and the output $V2 = \sqrt{\sum_{i=1}^{N} \phi_i^2}$ in ordinates axes, each one normalised to the number of oscillators.
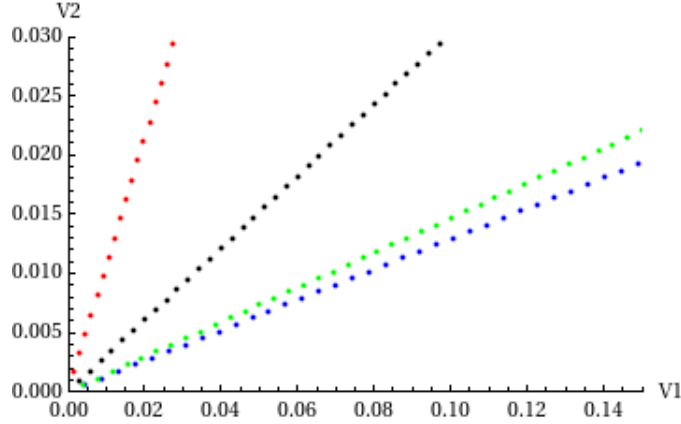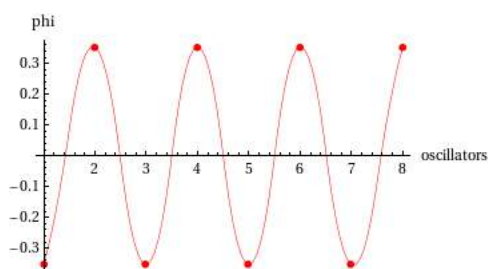

Figure 4.7: *Ring of 9 oscillators with nearest-neighbour coupling. Give an eigenvector, say the associated with the largest eigenvalue of the laplacian of the ring, we iterate it with a step of 0.02, and obtained the blue curve. The red curve is the iteration of the eigenvector associated with the lowest eigenvalue, and the other two curves are the eigenvectors associated with the intermediate eigenvalues.*

Some remarks are necessary at this point. In our work we use, as models to get insight in the behaviour of the system, rings with number of oscillators that go from 5 to 9, and even 11. We did not, as expected, see any difference but computational time consuming. However we must remark that the symmetries of eigenvectors of laplacians of odd and even number of oscillators are different. With 30 oscillators we can get some results that are equal but at the expense of a prohibitive computational time.

In the linear approximation, as we saw in chapter 4.2, the eigenvectors of the Laplacian of the graph with a finite number of oscillators are fixed points of the system. Their importance becomes patent when, on one hand we found that the eigenvector associated with the lowest eigenvalue, other than zero, is the upper bound of stable fixed points, that we can obtain solving Eq.(4.9) and the eigenvector associated with the eigenvalue is the lower bound to the stable fixed points, as shown in Fig.(4.7) and (4.8). On the other hand, we find that exists a bijection between the phase portrait obtained using the eigenvector associated with the larger eigenvalue and the phase portrait that we get with a frequency assignment with the greatest asymmetry, $(0, -1, 0, -1, 0, -1, 0, -1)$.

The same bijection, as we can see in figures (4.9) through (4.12) happens with the eigenvector associated with the lowest eigenvalue that is different from zero, and a frequency assignment with great symmetry, of the kind: $(a, b, a, c, -a, -b, -a, c)$.
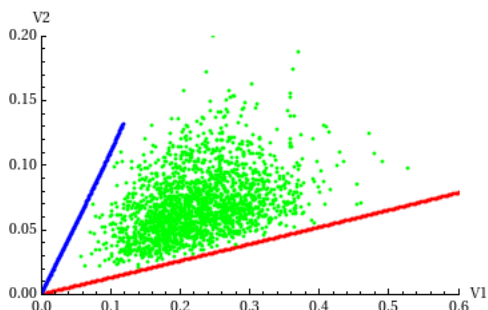
Figure 4.8: *Ring of 9 oscillators with nearest-neighbour coupling. Fixed points found solving Eq.4.9. We use a iteration of the eigenvectors associated with the largest and lowest eigenvalues of the Laplacian graph, and a random generation of 5000 vectors from a Gaussian distribution $N(0, 0.5)$.*
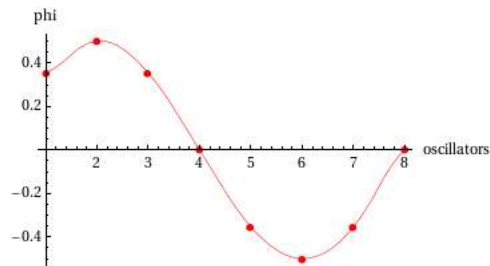

Figure 4.9: *Ring of 8 oscillators with nearest-neighbour coupling. Plot of the eigenvector associated with the largest eigenvalue of Laplacians' graph.*

Other feacture of the system under study emerge from Eq.4.9 itself. Remembering the
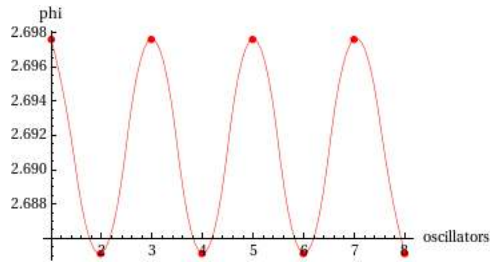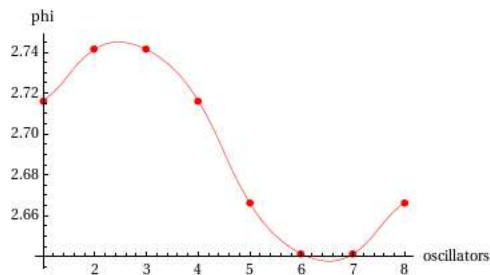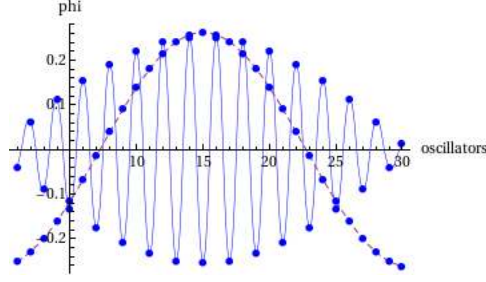
Figure 4.10: *Ring of* 8 *oscillators with nearest-neighbour coupling. Fixed points found solving the dynamic equations. As frequency distribution we use the vector (0,-1,0,-1,0,-1,0,-1) with variations along all vector* .

Figure 4.11: *Ring of* 8 *oscillators with nearest-neighbour coupling. Plot of the eigenvector associated with the lowest eigenvalue of Laplacians' graph* .

Figure 4.12: *Ring of* 8 *oscillators with nearest-neighbour coupling. Fixed points found solving the dynamic equations. As frequency distribution we use the vector (0,0,0,0,-1,-1,-1,-1) which concentrate all variation in one point* .

35

Figure 4.13: *Ring of* 30 *oscillators with nearest-neighbour coupling. Plot of the eigenvectors of the graph associated with the largest (asymmetric curve) and lowest eigenvalue .*

equation, $\delta_i + K[\sin(\phi_{i+1}) + \sin(\phi_{i-1}) - 2\sin\phi_i] = 0$ with the condition $\sum_{i=1}^{N}\phi_i = 0\,(\mathrm{mod}\,2\pi)$ we get that for sufficiently small δ_i, we get

$$\begin{cases} \sin(\phi_{i+1}) + \sin(\phi_{i-1}) - 2\sin\phi_i = 0, & i = 1, ..., N \\ \sum_{i=1}^{N}\phi_i = 0\,(\mathrm{mod}\,2\pi) \\ \phi_{N+1} = \phi_1 \end{cases} \qquad (4.10)$$

Implying

$$\begin{cases} \sin\phi_i = \frac{1}{2}[\sin(\phi_{i+1}) + \sin(\phi_{i-1})], & i = 1, ..., N \\ \sum_{i=1}^{N}\phi_i = 0\,(\mathrm{mod}\,2\pi) \\ \phi_{N+1} = \phi_1 \end{cases}$$

And since, on on hand $-1 \leq \sin\phi_i \geq 1$ and on the other each ϕ_i have two possible combinations of ϕ_{i+1} and ϕ_{i-1} we have two stable solutions as can be seen in Fig. (4.14) and (4.15)

4.3.2   Remarks on some results

What we have accomplished

Throughout our work we proceed along with the fruitfully way of theoretical insights gained by numerical results, and new ideas to numerical exploration gained by theoretical ideas. In working out we found more and more questions that must be addressed.

At this point we can tell, with a certain degree of certainty, that given a vector of frequencies and a ring of, e.g., 30 oscillators, say something about if it would synchronize, and if it synchronize, in what region of our space $(V1, V2)$ we will found ϕ.

Lets consider the graph and the eigenvalues and associated eigenvectors of its Laplacian. If $V1$ of a given vector is lower than the $V1$ found through the eigenvector associated with
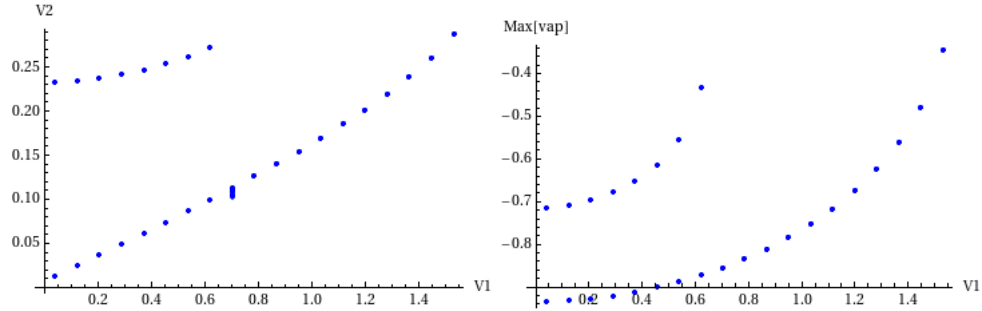
Figure 4.14: *Ring of* 9 *oscillators with nearest-neighbour coupling. In the left graph: Fixed points found solving Eq.4.9. Iteration of the eigenvector associated with the lowest eigenvalue of the Laplacian graph. In the right graph: Control over the great eigeivalue of the linearised matrix to ensure in each iteration that he is negative .*
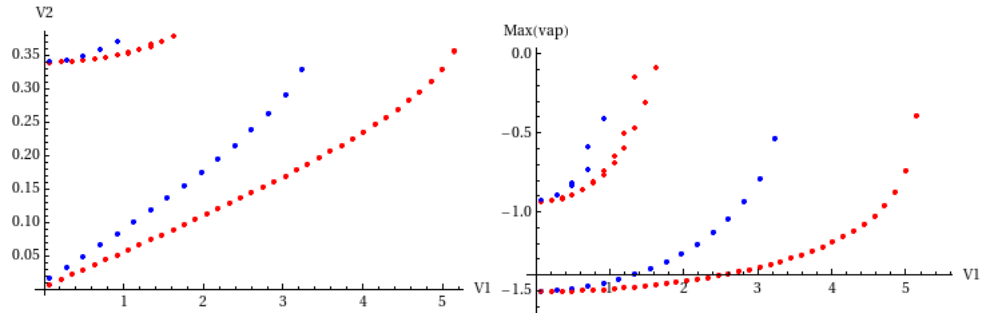

Figure 4.15: *Ring of* 7 *oscillators with nearest-neighbour coupling. In the left graph: Fixed points found solving Eq.4.9. Iteration of the eigenvectors associated with the lowest (blue) and larger (red) eigenvalues of the Laplacian graph. In the right graph: Control over the great eigenvalues of the linearised matrix to ensure in each iteration that they are negative .*

the maximum eigenvalue and greater than the $V1$ calculated with the eigenvector associated with the lowest eigenvalue, we can conclude, if $V1$ is *not to large* that it would synchronize.

Moreover we can tell, given two vectors and analysing their symmetry, the relation between their output $V2$ in $(V1, V2)$ space. The vector with lower $V2$, approaching the eigenvector associated with the largest eigenvalue would be the one with great asymmetry.

problems to explore

In our work we were not able to define a region in $(V1, V2)$ space that bound all vectors that would synchronize, given a definite topology and a coupling constant K.

Although we have gained a good insight on the behaviour of the system we did not explore how the variation on the coupling constant would be seen in the space we choose to work.

We ended without exploit other couplings than nearest-neighbours in a ring and, only in the beginning we saw some others topologies. Moreover the non linear region need to be carefully exploited.

Finally it will be useful, at least to a better understanding of the system, how other spaces other than $(V1, V2)$, namely $(W1, W2)$, with $W1 = \sqrt{\sum_{i=1}^{N} Max(\delta_i)}$, and $W2 = \sqrt{\sum_{i=1}^{N} Max(\phi_i)}$ would lead us to different approaches.

Chapter 5

Conclusions

The emergent properties shown by a system of phase coupling oscillators with a structured coupling are a rich and dynamic subject of active research. The rationale presented by most researchers in this area are biological processes. From cells to the realm of biological organs research in chains of phase coupled oscillators are an active field.

We did not find such a rationale in the research on rings of coupled oscillators. However the difference between chains and rings are only on the boundary conditions. We have seen that chains and rings of coupled oscillators are very sensitive to distributions of proper frequencies. If we take the distributios of proper frequencies to be the initial conditions of our systems, is expected that, to a certain extent, biological systems evolve in order to adjust these distributions to attain a better or easier synchronization. In fact we have seen a wide range of possibilities such as synchronization of frequencies, synchronization of frequencies and phases, different spatial patterns of synchronization and synchronization with phase locking but with a spatial split, named quimeras.

Is expected that biological oscillators in the evolutionary process could adjust their *initial conditions* in such a way that this adjustment leads the system to one state or another. We can mention some analogous processes in human behaviour:

The formation of rhythmic applause. This synchronization process in the concert hall offers a wonderful example of social self-organisation. In [31] one of the conclusions is that synchrony is a voluntary act of the individuals;

In some sporting activity as gymnastics, or swimming, synchronous movements are required in order to enhance performance. Sportsmen are trained to adjust their rhythms allowing synchronization.

The circadian rhythms. These processes are characterised by a period of about 24-hours, and are generated in nearly all living organisms. Macroscopically, we can say that there exists synchrony between human physiology and the world around us acting as a master oscillator [2]. Under normal conditions of living on a regular schedule, seeing sunlight, sleeping at night, and so on, the entire body is synchronized to the 24-hours day, driven

mainly by the cycle of light and darkness. A change in these habits can perturb this synchronous behaviour and manifestations such as sleep or digestive troubles are observed especially when we change time zones in long-distance travel.

So is expected that this sensitivity to proper frequencies distributions in rings of phase coupled oscillators induces some changes in proper frequencies of cells or individual in order to attain the desired pattern.
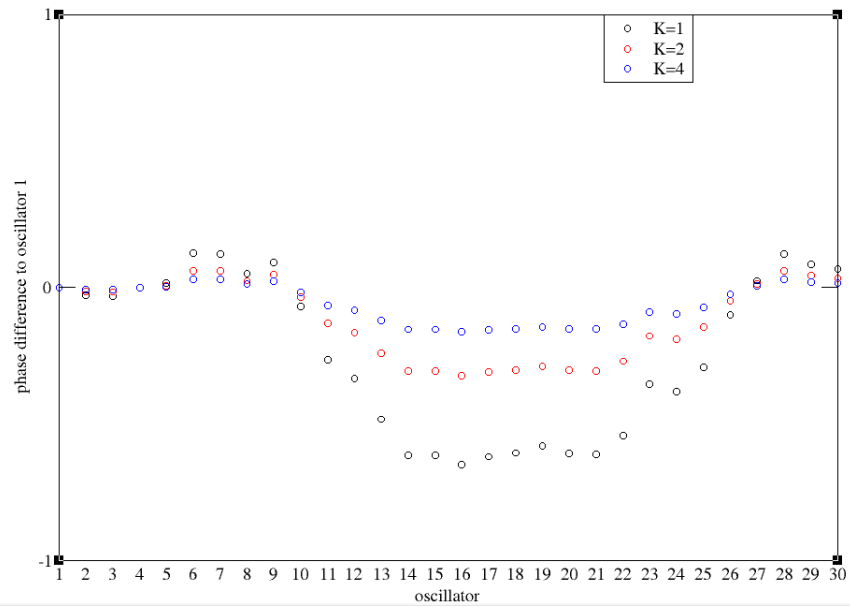
Appendix A

Figure A.1: *Circle with nearest-neighbour coupling. Integration of Eq.2.1 with* 30 *oscillators. Frequency distribution* $N(2, 0.1)$. *Variation of the coupling constant and its effect on phase distribution.*
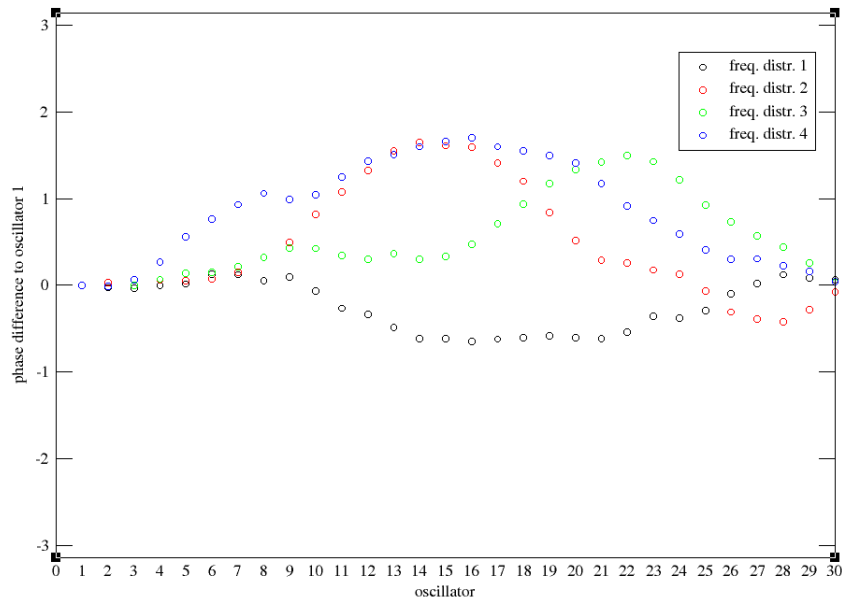
Figure A.2: *Circle with nearest-neighbour coupling. Integration of Eq.2.1 with* 30 *oscillators. Variation of the frequency distribution and its effect on phase distribution. All frequency distribution comes from* $N(2, 0.1)$.
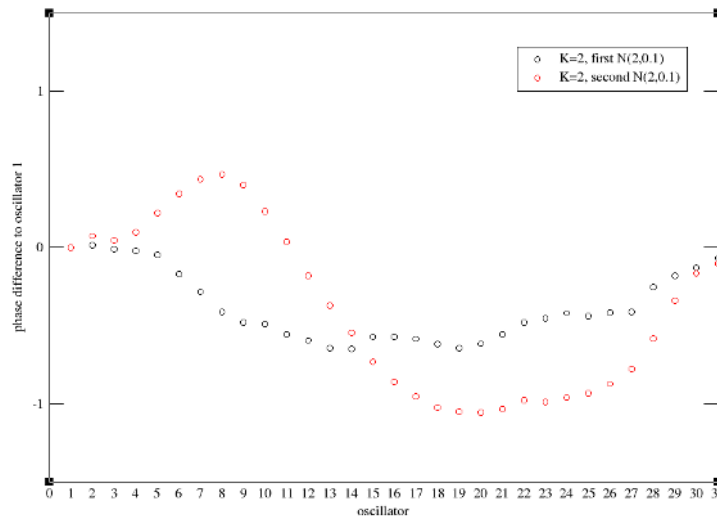
Figure A.3: *Circle with nearest-neighbour coupling. Integration of Eq.2.1 with* 31 *oscillators. Two different frequencies distribution* $N(2, 0.1)$. *We can see, as expected, that* 30 *oscillators is not a singular case.*
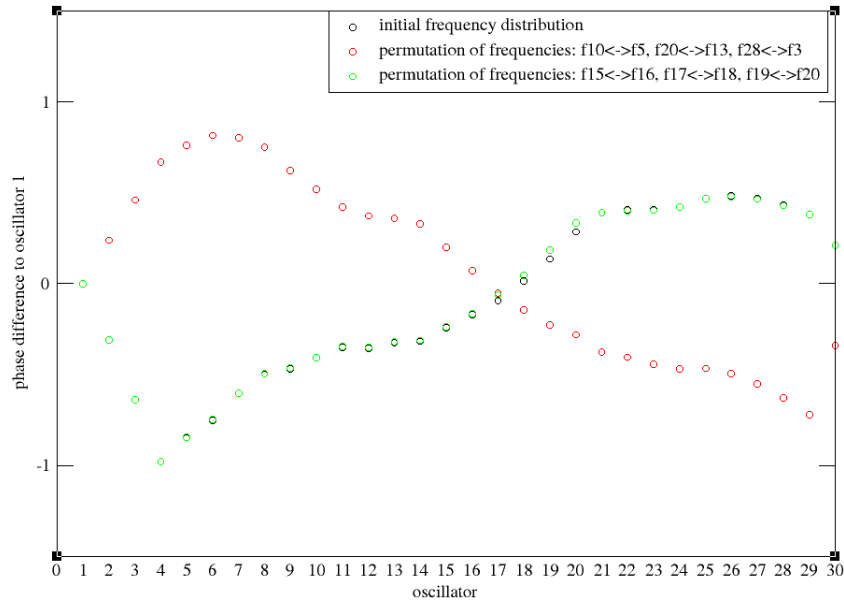
Figure A.4: *Circle with nearest-neighbour coupling. Integration of Eq.2.1 with* 30 *oscillators. K=2. Effect of frequency permutations.*
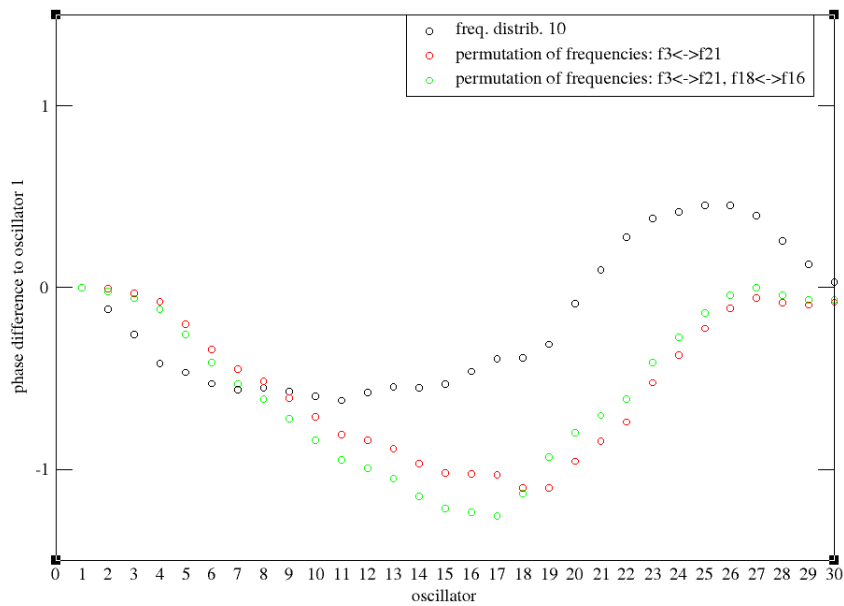
Figure A.5: *Circle with nearest-neighbour coupling. Integration of Eq.2.1 with* 30 *oscillators. K=2. Effect of frequency permutations.*
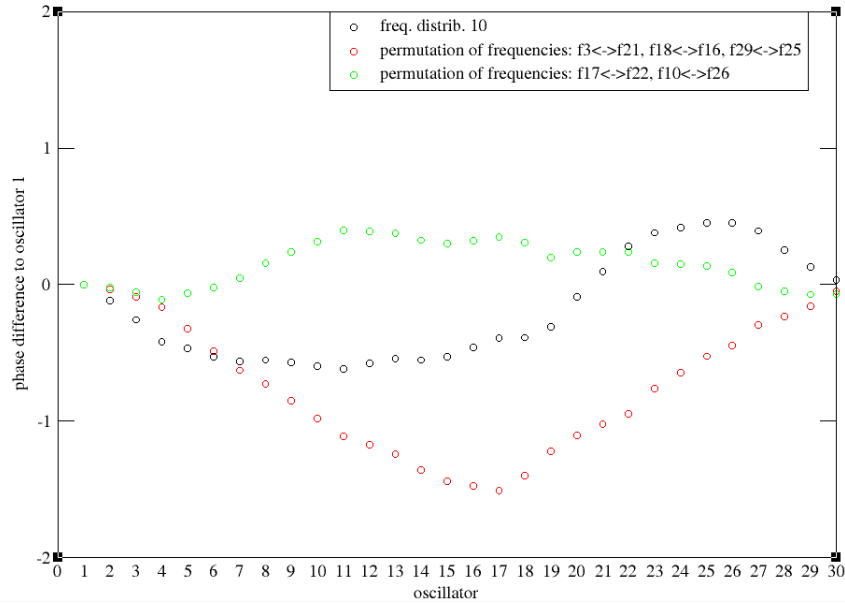
Figure A.6: *Circle with nearest-neighbour coupling. Integration of Eq.2.1 with* 30 *oscillators. K=2. Effect of frequency permutations.*
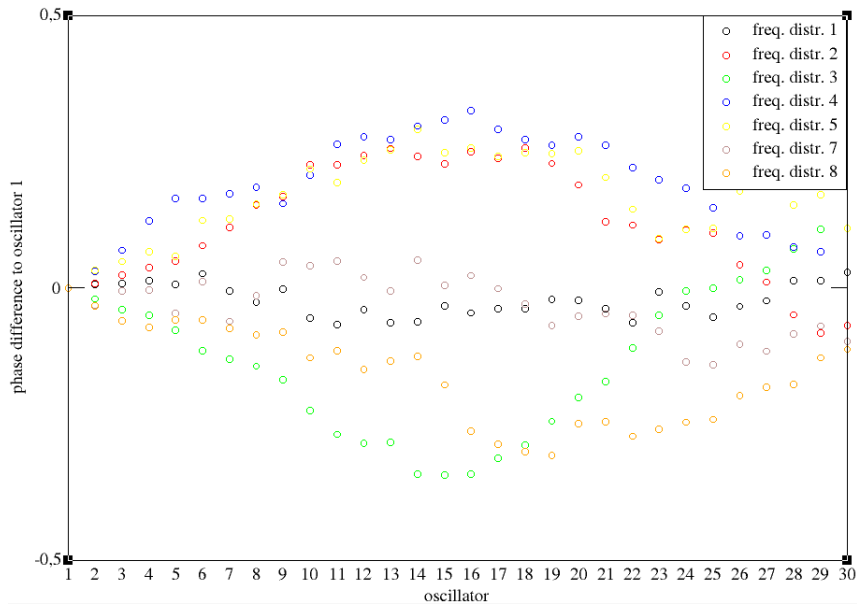

Figure A.7: *Chain of* 30 *oscillators with unidirectional nearest-neighbour coupling. Integration of Eq.2.1. Effect of frequency permutations.*
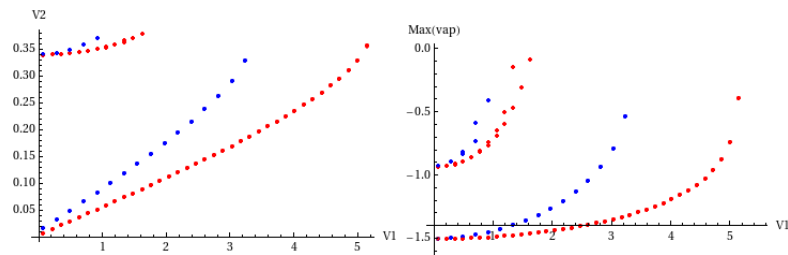
Appendix B

Figure B.1: *Ring of 7 oscillators with nearest-neighbour coupling. In the left graph: Fixed points found solving Eq.4.9. Iteration of the eigenvectors associated with the lowest (blue) and largest (red) eigenvalues of the Laplacian graph. In the right graph: Control over the largest eigenvalues of the linearised matrix to ensure in each iteration that they are negative* .
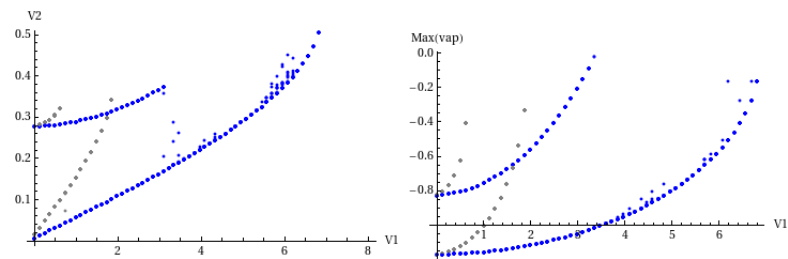

Figure B.2: *Ring of 8 oscillators with nearest-neighbour coupling. In the left graph: Fixed points found solving Eq.4.9. Iteration of the eigenvectors associated with the lowest (blue) and largest (red) eigenvalues of the Laplacian graph. In the right graph: Control over the largest eigenvalues of the linearised matrix to ensure in each iteration that they are negative* .
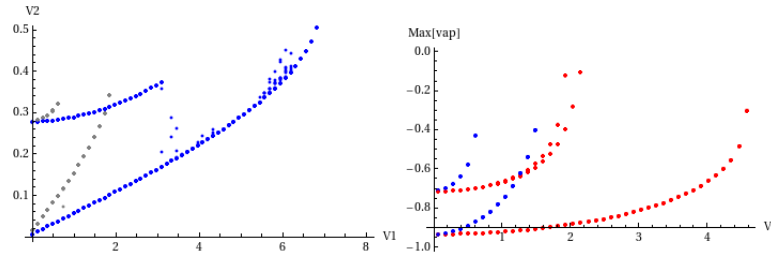
Figure B.3: *Ring of 9 oscillators with nearest-neighbour coupling. In the left graph: Fixed points found solving Eq.4.9. Iteration of the eigenvectors associated with the lowest (blue) and largest (red) eigenvalues of the Laplacian graph. In the right graph: Control over the largest eigenvalues of the linearised matrix to ensure in each iteration that they are negative .*
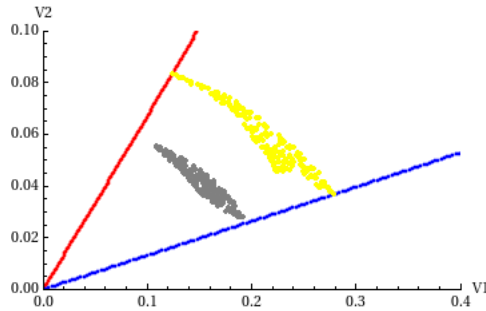

Figure B.4: *Ring of 7 oscillators with nearest-neighbour coupling. Fixed points found solving Eq.4.9. Iteration of the eigenvectors associated with the lowest (red) and largest (blue) eigenvalues of the Laplacian graph. Overlap of all different permutations of both eigenvectors (yellow). Permutation of a vector N(0,0.3) (gray) .*
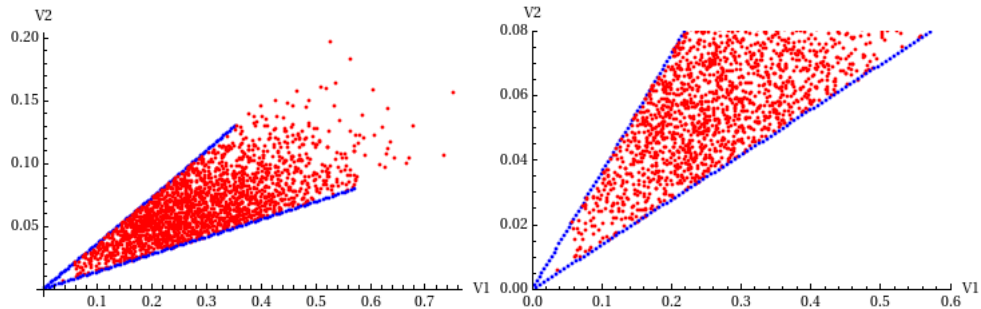

Figure B.5: *Left graph: Ring of 5 oscillators with nearest-neighbour coupling. Fixed points found solving Eq.4.9. Iteration of the eigenvectors associated with the lowest and largest (blue) eigenvalues of the Laplacian graph. 2000 outputs of a N(2, 0.5) (red). Right graph: enlargement of the left graph .*

Bibliography

[1] A. Pikovski, M. Rosenblum and J. Kurths. *Synchronization, A universal concept in nonlinear sciences.* Cambridge University Press, (2001).

[2] S.H. Strogatz. *Sync: The Emerging Science of Spontaneous Order.* Hyperion, (2003).

[3] A.T. Winfree. *The Geometry of Biological Time.* Springer, New York, 2nd ed. (2001).

[4] A. A. Andronov, S.E. Khaikin. *Theory of Oscillations.* Princeton University Press, (translated and adopted by S. Lefshetz from the first edition in 1937), (1949).

[5] N. Wiener. *Cybernetics: Or Control and Communication in the Animal and the Machine.* MA: MIT Press.Cambridge, (1948).

[6] S. H. Strogatz. From Kuramoto to Crawford: Exploring the onset of synchronization in populations of coupled oscillators. *Physica D*, **143** 1-20 (2000).

[7] I. Mihalcescu, W. Hsing and S. Leibler. Resilient circadian oscillator in individual cyanobacteria. *Nature*, **430**, 81-85 (2004).

[8] D. A. Wiley and S. H. Strogatz. newblock The size of the sync basin. *Chaos*, **16**, 015103
(2006).

[9] C. J. Perez Vicente F. Ritort J. A. Acebron, L. L. Bonilla and R. Spigler. The Kuramoto model: A simple paradigm for synchronization phenomena. *Rev. Mod. Phys.*, **77** (2005).

[10] S. Wiggins. *Introduction to Applied Nonlinear Dynamical Systems and Chaos.* Springer-Verlag, (1990).

[11] Y. Kuramoto. *Chemical oscillations, waves and turbulence.* Springer-Verlag, Berlin (1984).

[12] Y. Kuramoto. Statistical Macrodynamics of Large Dynamical Systems. Case of a Phase Transition in Oscillator Communities. *Journal of Statistical Physics*, **49** (1987).

[13] R. E. Mirollo and S. H. Strogatz. The spectrum of the partially locked state for the Kuramoto model. *J. Nonlinear Sci.* **17**, 309-347 (2007).

[14] R. E. Mirollo and S. H. Strogatz. The spectrum of the locked state for the Kuramoto model of coupled oscillators. *Physica D* **205**, 249-266 (2005).

[15] E. Ott and T. M. Antonsen. Low dimensional behaviour of large systems of globally coupled oscillators. *Chaos* **18**, 037113 (2008).

[16] E. Ott and T. M. Antonsen. Long time evolution of phase oscillator systems. *Chaos* **19**, 023117 (2009).

[17] D. M. Abrams and S. H. Strogatz. Chimera states for coupled oscillators. *Phys. Rev. Lett.* **93** 17 (2004).

[18] Y. Kuramoto and D. Battogtokh. Coexistence of coherence and incoherence in nonlocally coupled phase oscillators: A soluble case. *Nonlinear Phenom. Complex Syst.* **5**, 380 (2002).

[19] D. M. Abrams and S. H. Strogatz. Chimera states in a ring of nonlocally coupled oscillators. *International Journal of Bifurcation and Chaos*, **16** 21-37 (2006).

[20] D. J. Watts and S. H. Strogatz. Collective dynamics of 'small-world' networks. *Nature* **393**, 409-410 (1998).

[21] D. J. Watts. *Small Worlds.* Princeton University Press, Princeton (1999).

[22] A.- L. Barabási and R. Albert. Emergence of scaling in random networks. *Science,* **286**, 509-512 (1999).

[23] G.V. Osipov, J. Kurths and C. Zhou. *Synchronization in Oscillatory Networks.* Springer-Verlag, (2007).

[24] G.B. Ermentrout and N. Koppel. Frequency plateaus in a chain of weakly coupled oscillators,I. *SIAM J. Math. Anal,* **15**, 215-237 (1984).

[25] G.B. Ermentrout and N. Koppel. Symmetry and phase-locking in chains of weakly coupled oscillators. *Comm. Pure Appl. Math.* **39**, 623-660 (1986).

[26] G.B. Ermentrout and N. Koppel. Oscillators death in systems of coupled neural oscillators. *SIAM J. Appl. Math.,* **50**, 125-146 (1990).

[27] N. Koppel, W. Zang and G.B. Ermentrout. Multiple coupling in chains of oscillators. *SIAM J. Math. Anal.,* **21**, 935-953 (1990).

[28] A.Pikovsky and P. Rosenau. Phase Compactons. *Physica D,* **218**, 56-69 (2006).

[29] D. Aeyels and A. Rogge. Existence of partial entrainment and stability of phase locking behavior of coupled oscillators. *Progress of Theoretical Physics* **112**, 921-946 (2004).

[30] Filip De Smet and D. Aeyeles. Partial entrainment in the finite Kuramoto-Sakaguchi model. *Physica D* **234**, 81-89 (2007).

[31] Z. Néda, E. Ravasz, T. Vicsek, Y. Brecht and A.L. Barabási. Physics of rhythmic applause. *Phys. Rev. E.* **61**, 6987-6992 (2000).

[32] Yu. Maistrenko, O. Popovych, O. Burylko and P.A. Tass. Mechanism of Desynchronization in the finite-Dimensional Kuramoto Model. *Phys. Rev. Lett.* **93**, N.8 (2004).

[33] L. Mendelowitz, A. Verdugo and R. Rand. Mechanism of Desynchronization in the finite-Dimensional Kuramoto Model. *Communications in Nonlinear Science and Numerical Simulation.* **93**, 270-283, 14 (2009).

[34] B. Ermentrout. *Simulating, analysing, and Animating Dynamical Systems - A guide to XPPAUT for researchers and students.* SIAM, Philadelphia (2002).

[35] W.N. Anderson,JR. and T.D. Morley. Eigenvalues of the Laplacian of a Graph. *Linear and Multilinear Algebra.* **18**, 141-145, (1985).